Mathematical Biosciences and Engineering

https://www.aimspress.com/journal/mbe

MBE, 23(8): 2367–2392.
DOI: 10.3934/mbe.2026086
Received: 27 March 2026
Revised: 21 May 2026
Accepted: 10 June 2026
Published: 30 July 2024

Research article

Dynamics of a network-based SIR epidemic model with double impulsive controls

Gui Guan[1,2], Zhenyuan Guo[1*], Yanyu Xiao[3] and Yuming Chen[4]

[1] School of Mathematics, Hunan University, Changsha 410082, China
[2] Faculty of Mathematics and Physics, Huai'an University, Huai'an 223003, China
[3] Department of Mathematical Sciences, University of Cincinnati, Cincinnati, OH 45221, USA
[4] Department of Mathematics, Wilfrid Laurier University, Waterloo, Ontario, N2L 3C5, Canada

* **Correspondence:** Email: zyguo@hnu.edu.cn.

Abstract: A network-based susceptible-infected-recovered (SIR) epidemic model is proposed to study the spread of infectious diseases, thereby incorporating vertical transmission and a saturated incidence rate. Additionally, it introduces double impulsive control strategies, including pulse vaccination and screening with treatment at distinct fixed intervals. Dynamical behaviors of the formulated model are analyzed using two types of transmission thresholds, namely $R^0_{k_i}$ and $\widehat{R^0_{k_i}}$. By applying the Floquet theorem and comparison principle, the system admits a disease-free periodic solution that is globally asymptotically stable if $\max\limits_{i=1,2,\ldots,n} \widehat{R^0_{k_i}} < 1$. The persistence of disease is confirmed from the uniform persistence of the Poincaré map when $\frac{1}{1+\alpha} \max\limits_{i=1,2,\ldots,n} R^0_{k_i} > 1$, where α is the saturated coefficient in the saturation infection. Scenario studies are performed to numerically evaluate the impact of various parameters on the disease dynamics, and the effectiveness of double impulsive controls. It can be concluded that synthetical double impulsive controls are more efficient at eradicating the disease compared with only either of them.

Keywords: complex network; disease modeling; pulse; stability; uniform persistence

1. Introduction

Mathematical modeling serves as a powerful tool for providing theoretical support in examining the disease transmission progress and assessing disease control and prevention strategies from various perspectives [1, 2]. Numerous mathematical models with different focuses have been developed and analyzed to study the epidemic dynamics in the past decades. Zhang and Xu [3] studied the global stability of both disease-free and endemic steady states for a diffusive epidemic model with a Beddington-

DeAngelis functional response. In [4], Khan et al. found the existence of backward bifurcations from an epidemic model that incorporated different phases of hepatitis B by considering migration, hospitalization, and vaccination. By utilizing the fractional Barbalat's Lemma, Karaji and Nyamoradi [5] analyzed the global dynamics of an epidemic model formulated with a fractional derivative. Hussain et al. [6] developed a stochastic epidemic model with double saturated incidence rates, and examined the conditions for disease extinction and the existence of ergodic stationary distributions by constructing an appropriate stochastic Lyapunov function. In [7], Raezah et al. analyzed the long-term behavior of disease dynamics by performing an optimal control and stability analysis on an epidemic model that differentiates between acute and chronic carrier individuals.

Network science has become a crucial paradigm for revealing fascinating insights into the spread and dispersal of infectious diseases within heterogeneous populations in the era of big data [8, 9]. In recent decades, modeling efforts have explored infectious diseases using network frameworks, thereby incorporating effective contact rates in heterogeneous populations [10–14]. Cao et al. [10] built a homogeneous epidemic model on a network-structured population considering various states of carriers. Wu et al. [11] illustrated the global stability of the co-existence equilibrium for a two-strain epidemic network model with immunity waning and imperfect vaccination. An optimal control strategy, aiming at jointly optimizing the least robustness and highest convergence rate, was investigated for a susceptible-infectious-susceptible (SIS) network model with time delay in [12]. Utilizing the microscopic Markov chain approach, Lv et al. [13] proposed a novel Unawareness-Awareness-Unawareness-SIS epidemic model with a two-layer network structure to investigate the dynamics of epidemic spreading coupled with the diffusion of awareness in the population. Oestereich et al. [14] explored the critical impact of network structure on epidemic transmissions by an adaptive network model that incorporated the intricate interactions among vaccination strategies, human dispersal, and opinion dynamics.

To better mimic the practical implementation of control measures, impulsive interventions have been widely adopted and analyzed across various domains. They have proven effective in managing infectious diseases [15–18], mitigating rumor propagation [19, 20], and controlling pest populations [21, 22]. For example, the state-dependent impulsive control was embedded in two classical susceptible-infectious-recovery (SIR) models with media coverage [1] and saturation incidence [23]. Fu et al. [15] proposed and analyzed a susceptible-asymptomatic-infectious-quarantine-recovery (SAIQR) epidemic model with non-instantaneous pulse vaccination on some complex networks. Zhang et al. [16] identified the presence of a backward bifurcation in a state-dependent impulsive SIR model that incorporated feedback control strategies, which encompass vaccination, isolation, and treatment. Jiang et al. [17] discussed the existence of periodic solutions for an SIS epidemic model with fixed-time pulse births and state-dependent pulse treatments. In the hybrid SIR model proposed by Li and Xiao [18], the decision to implement pulse vaccination and isolation hinges on the susceptible population size. Liu and Stechlinski employed pulse vaccination and treatment on an SIR epidemic model [24] and a switched multi-city SIR epidemic model [25] featuring time-varying contact rate, respectively.

Real-world social contact networks are inherently heterogeneous. Moreover, many infectious diseases are controlled through periodic vaccinations and treatment campaigns. Coordinating these two interventions can significantly reduce the disease burden. Therefore, it is essential to investigate the dynamics and control strategies of network-based epidemic models by incorporating multiple pulse controls. In this work, based on complex networks, we will explore the transmission dynamics of an

SIR epidemic model by incorporating both impulsive vaccinations and screenings with treatments. Our study will assess the effectiveness of two pulse control strategies in addressing two distinct pathogen transmission mechanisms on complex networks. It is worth mentioning that the proposed model reveals that vertical transmission increases the persistence threshold, meaning that diseases with vertical transmission require stronger impulsive controls to eradicate. This is a practically relevant finding for public health. The main contributions of this paper are as follows:

- While most existing studies only consider a single impulsive control, we propose a novel network-based epidemic model with vertical transmission, saturated incidence, and a double impulsive strategy that combines pulse vaccinations and screenings with treatments.
- Using the Floquet theory, comparison principles, and Poincaré map methods on a high-dimensional coupled model, we obtain the transmission threshold, the existence and stability of disease-free periodic solution, and the sufficient condition for the uniform persistence of disease.

The structure of this paper is as follows: in Section 2, we formulate our network-based SIR epidemic model; Section 3 presents the well-posedness of the solutions and derives two types of transmission thresholds, along with other theoretical results on the dynamics of the proposed model; in Section 4, numerical simulations are provided to illustrate the theoretical findings from Section 3; and finally the paper concludes with a discussion in Section 5.

2. Model formulation

We develop our model for the epidemic transmission on top of a social contact network. Assume that the population is conserved and divided into three compartments: susceptible, infected, and recovered. The heterogeneity in the population is represented by the structure of a predefined network. Each node in the contact network corresponds to an individual, while an edge between two nodes signifies a connection between them. In the current work, we adopt a degree-based mean-field approach, where all nodes with the same degree are assumed to exhibit identical dynamical behaviors. Generally speaking, a node-level approach for epidemic modeling in complex networks can capture finer individual heterogeneity, local structural details, and node-specific intervention priorities. However, such a model would be significantly more complex to analyze, especially in the presence of double impulsive controls. For large uncorrelated networks, the degree-based aggregation provides an analytically tractable approximation, thus enabling us to derive the transmission threshold, system stability, and persistence conditions. These theoretical insights are the primary goals of this study. The degree-level abstraction retains the essential heterogeneity due to degree differences, which is often sufficient to capture the overall epidemic dynamics and evaluate the effectiveness of impulsive control strategies. The trade-off is therefore between analytical depth and microscopic detail; for the present purpose, the degree-based formulation is a reasonable and powerful choice. The connectivity of an individual is quantified by the degree of a node, denoted as $k_i, i = 1, 2, \ldots, n$, which represents the number of neighbors each individual has. The maximum possible number of neighbors for any individual is set to n. Consequently, the population on the network is categorized into $3n$ groups, representing three epidemiological states with contact numbers ranging from 1 to n. We further define $S_{k_i}(t)$, $I_{k_i}(t)$, and $R_{k_i}(t)$ as the densities of susceptible, infected, and recovered individuals with degree k_i at time t, respectively.

Since we assume that the birth rate is the same as the death rate, we get a conservative system and have $\mu(S_{k_i}(t) + I_{k_i}(t) + R_{k_i}(t)) = \mu$ account for the newborns. Denote $1 - \delta$ as the probability

of disease pathogen transmitted vertically from an infectious mother to a newborn. Then the term $(1-\delta)\mu I_{k_i}(t)$ is used to characterize the density of newly infected individuals within a unit of time due to vertical transmission, which needs to be subtracted from the total newborn to susceptible population. Additionally, susceptible individuals with k_i neighbors could catch this disease pathogen by contacting infected individuals at the rate of $\lambda(k_i)$. Denote $p(k_i)$ as the distribution of nodes in the network, which meets $\sum_{i=1}^{n} p(k_i) = 1$. Moreover, $\langle k_i \rangle = \sum_{i=1}^{n} k_i p(k_i)$ is the average degree of the network. Thus, the average infectivity exposed to individuals in S_{k_i} is

$$\Theta(t) = \sum_{i=1}^{n} \omega(k_i) p(k_i) I_{k_i}(t) / \langle k_i \rangle,$$

or interpreted as the average infectivity exposed via one edge of a node in $S_{k_i}(t)$, where $\omega(k_i)$ is the average infectivity of an infected individual with k_i neighbors, and $\omega(k_i)$ is assumed to be less than k_i for all i following the argument in [26]. Furthermore, we consider a saturated infectivity by contacting infected individuals in the neighborhood by bringing in α, a saturated coefficient, to formulate the saturated average infectivity $\frac{\Theta(t)}{1+\alpha\Theta(t)}$. Finally, we derive the force of infection as $\lambda(k_i) S_{k_i}(t) \frac{\Theta(t)}{1+\alpha\Theta(t)}$, which reflects the disease pathogen dispersal over a network setting.

Following the idea in [27], we develop an SIR epidemic model on a complex network with the periodic occurrence of both vaccination and screening with treatment. Assume that susceptible individuals with degree k_i are inoculated against the disease pathogen in an impulsive and period manner, by a fixed proportion q_i each time $t = mT, m \in \mathbb{Z}^+ = \{1, 2, 3, \ldots\}$. Additionally, infected individuals are subjected to a therapy service at set intervals, with the same period as the action of vaccination but at different moments. γ_i is the cure rate of infected individuals with degree k_i at time $t = (m+l-1)T, m \in \mathbb{Z}^+, 0 < l < 1$. T is the period of impulsive control measures. All system parameters are supposed to be positive.

Based on the above assumptions and transition rules, we establish a network-based SIR epidemic model which incorporates vertical transmission, saturated incidence, pulse vaccination, and screening with treatment. The model is formulated using the following impulsive differential equations:

$$\begin{cases} \left.\begin{aligned} &\frac{\mathrm{d}S_{k_i}(t)}{\mathrm{d}t} = \mu - (1-\delta)\mu I_{k_i}(t) - \lambda(k_i) S_{k_i}(t) \frac{\Theta(t)}{1+\alpha\Theta(t)} - \mu S_{k_i}(t), \\ &\frac{\mathrm{d}I_{k_i}(t)}{\mathrm{d}t} = (1-\delta)\mu I_{k_i}(t) + \lambda(k_i) S_{k_i}(t) \frac{\Theta(t)}{1+\alpha\Theta(t)} - rI_{k_i}(t) - \mu I_{k_i}(t), \\ &\frac{\mathrm{d}R_{k_i}(t)}{\mathrm{d}t} = rI_{k_i}(t) - \mu R_{k_i}(t), \end{aligned} \right\} \begin{aligned} &t \neq (m+l-1)T, \\ &t \neq mT, \end{aligned} \\ \left.\begin{aligned} &S_{k_i}(t^+) = S_{k_i}(t), \\ &I_{k_i}(t^+) = (1-\gamma_i) I_{k_i}(t), \\ &R_{k_i}(t^+) = R_{k_i}(t) + \gamma_i I_{k_i}(t), \end{aligned} \right\} t = (m+l-1)T, \\ \left.\begin{aligned} &S_{k_i}(t^+) = (1-q_i) S_{k_i}(t), \\ &I_{k_i}(t^+) = I_{k_i}(t), \\ &R_{k_i}(t^+) = R_{k_i}(t) + q_i S_{k_i}(t), \end{aligned} \right\} t = mT, \end{cases} \tag{2.1}$$

where $t > 0$, $i = 1, 2, \ldots, n$, and $0 < \gamma_i, q_i < 1$. The initial condition of System (2.1) is as follows:

$$S_{k_i}(0^+) = S_{k_i,0} \geq 0, I_{k_i}(0^+) = I_{k_i,0} \geq 0, R_{k_i}(0^+) = R_{k_i,0} = 1 - S_{k_i,0} - I_{k_i,0} \geq 0,$$

where $x(t_0^+) = \lim_{h \to 0^+} x(t_0 + h)$.

In System (2.1), the sum of $S_{k_i}(t)$, $I_{k_i}(t)$, and $R_{k_i}(t)$ remains constant, as the birth and death rates of individuals are balanced. Although the addition and removal of nodes may impact the network topology, their proportion is small in large-scale networks, which results in only minor structural changes [10]. In this manuscript, we focus on a static heterogeneous network with a constant size. Therefore, we eliminate the decoupled equation for $R_{k_i}(t)$ and study the following reduced system:

$$\begin{cases} \left.\begin{aligned} &\frac{\mathrm{d}S_{k_i}(t)}{\mathrm{d}t} = \mu - (1-\delta)\mu I_{k_i}(t) - \lambda(k_i)S_{k_i}(t)\frac{\Theta(t)}{1+\alpha\Theta(t)} - \mu S_{k_i}(t),\\ &\frac{\mathrm{d}I_{k_i}(t)}{\mathrm{d}t} = \lambda(k_i)S_{k_i}(t)\frac{\Theta(t)}{1+\alpha\Theta(t)} - rI_{k_i}(t) - \delta\mu I_{k_i}(t),\end{aligned}\right\} \begin{aligned} &t \neq (m+l-1)T,\\ &t \neq mT,\end{aligned}\\ \left.\begin{aligned} &S_{k_i}(t^+) = S_{k_i}(t),\\ &I_{k_i}(t^+) = (1-\gamma_i)I_{k_i}(t),\end{aligned}\right\} t = (m+l-1)T,\\ \left.\begin{aligned} &S_{k_i}(t^+) = (1-q_i)S_{k_i}(t),\\ &I_{k_i}(t^+) = I_{k_i}(t),\end{aligned}\right\} t = mT, \end{cases} \tag{2.2}$$

where $t > 0$, $i = 1, 2, \ldots, n$, and $0 < \gamma_i, q_i < 1$.

For convenience, we introduce the following notations: $\mathbb{R}_+ = [0, +\infty)$, $\mathbb{R}_+^{3n} = \{\mathbf{x} \in \mathbb{R}^{3n} \,|\, \mathbf{x} \geq 0\}$. Let f_i^S, f_i^I, and f_i^R be the map defined by the right-hand side of equations for $S_{k_i}(t), I_{k_i}(t)$, and $R_{k_i}(t)$, respectively. Denote $\mathbf{f} \triangleq (f_1^S, f_2^S, \ldots, f_n^S, f_1^I, f_2^I, \ldots, f_n^I, f_1^R, f_2^R, \ldots, f_n^R)^T$. The solution of System (2.1) is denoted as $\mathbf{x}(t) = (\mathbf{S}(t), \mathbf{I}(t), \mathbf{R}(t)) \triangleq \left\{(S_{k_i}(t), I_{k_i}(t), R_{k_i}(t))\right\}_{i=1}^n : \mathbb{R}_+ \to \mathbb{R}^{3n}$, where $\mathbf{S}(t) = (S_{k_1}(t), S_{k_2}(t), \ldots, S_{k_n}(t))$, $\mathbf{I}(t) = (I_{k_1}(t), I_{k_2}(t), \ldots, I_{k_n}(t))$, and $\mathbf{R}(t) = (R_{k_1}(t), R_{k_2}(t), \ldots, R_{k_n}(t))$. Let $\mathbf{x^0} = (S_{k_1,0}, S_{k_2,0}, \ldots, S_{k_n,0}, I_{k_1,0}, I_{k_2,0}, \ldots, I_{k_n,0})$ be the initial value of System (2.2).

3. Main results

3.1. Well-posedness of solutions and disease-free periodic solutions

A solution of System (2.1) is a function on $[0, t_{\max})$, which is continuously differentiable on $((m-1)T, (m+l-1)T] \times \mathbb{R}_+^{3n}$ and $((m+l-1)T, mT] \times \mathbb{R}_+^{3n}, m \in \mathbb{Z}^+, 0 < l < 1$, and $\mathbf{x}((m+l-1)T^+) = \lim_{t\to(m+l-1)T^+} \mathbf{x}(t), \mathbf{x}(mT^+) = \lim_{t\to mT^+} \mathbf{x}(t)$ exist such that System (2.1) is satisfied. With the nonnegative initial condition, System (2.1) has a unique solution existing globally, which is ensured by the smoothness properties of the map f. For details, see [28, 29].

Lemma 3.1. *For any given initial condition, the solution of System (2.1) satisfies* $\mathbf{x}(t) \geq 0$ *for all* $t > 0$. *Besides, all solutions of System (2.1) are in the following positively invariant set:*

$$\overline{\Omega} = \left\{ \left\{(S_{k_i}(t), I_{k_i}(t), R_{k_i}(t))\right\}_{i=1}^n \in \mathbb{R}_+^{3n} \,\middle|\, S_{k_i}(t) + I_{k_i}(t) + R_{k_i}(t) = 1,\ t > 0,\ i = 1, 2, \ldots, n \right\}.$$

Lemma 3.2. *[30]. The impulsive differential equation*

$$\begin{cases} \dfrac{\mathrm{d}u(t)}{\mathrm{d}t} = a - bu(t),\ t \neq mT, m \in \mathbb{Z}^+,\\ u(t^+) = (1-\theta)u(t),\ t = mT, m \in \mathbb{Z}^+, \end{cases} \tag{3.1}$$

where $a, b > 0, 0 < \theta < 1$, *has a unique positive periodic solution*

$$\overline{u}(t) = \frac{a}{b} + \left(u^* - \frac{a}{b}\right)e^{-b(t-mT)},\ mT < t \leq (m+1)T,$$

where $u^* = \frac{a}{b}\frac{(1-\theta)(1-e^{-bT})}{1-(1-\theta)e^{-bT}}$, *which is globally asymptotically stable.*

Based on the above Lemma 3.2, we obtain the existence of a disease-free periodic solution of System (2.2). Namely, there are no infected individuals in the social contact network.

Theorem 3.1. *There exists a disease-free periodic solution* $\mathbf{E_0}(t) = \left\{(S^T_{k_i}(t), 0)\right\}_{i=1}^n$ *of System (2.2), where*

$$S^T_{k_i}(t) = 1 - \frac{q_i e^{-\mu(t-mT)}}{1-(1-q_i)e^{-\mu T}},\ mT < t \le (m+1)T.$$

3.2. Global stability of the disease-free periodic solution

Theorem 3.2. *The disease-free periodic solution* $\mathbf{E_0}(t)$ *of System (2.2) is locally asymptotically stable if* $\max\limits_{i=1,2,\ldots,n} R^0_{k_i} < 1$, *where* $R^0_{k_i} = \frac{\lambda(k_i)\omega(k_i)p(k_i)}{\langle k_i\rangle\left[r+\delta\mu-\frac{1}{T}\ln(1-\gamma_i)\right]}\left[1-\frac{q_i(1-e^{-\mu T})}{T\mu[1-(1-q_i)e^{-\mu T}]}\right]$.

Proof. The linear approximation system of System (2.2) at $\mathbf{E_0}(t)$ is as follows:

$$\begin{cases} \left.\begin{aligned} &\frac{\mathrm{d}S_{k_i}(t)}{\mathrm{d}t} = -\mu S_{k_i}(t) - (1-\delta)\mu I_{k_i}(t) - \lambda(k_i)S^T_{k_i}(t)\Theta(t),\\ &\frac{\mathrm{d}I_{k_i}(t)}{\mathrm{d}t} = \lambda(k_i)S^T_{k_i}(t)\Theta(t) - (r+\delta\mu)I_{k_i}(t),\end{aligned}\right\} \begin{aligned} &t \ne (m+l-1)T,\\ &t \ne mT,\end{aligned}\\ \left.\begin{aligned} &S_{k_i}(t^+) = S_{k_i}(t),\\ &I_{k_i}(t^+) = (1-\gamma_i)I_{k_i}(t),\end{aligned}\right\} t = (m+l-1)T,\\ \left.\begin{aligned} &S_{k_i}(t^+) = (1-q_i)S_{k_i}(t),\\ &I_{k_i}(t^+) = I_{k_i}(t),\end{aligned}\right\} t = mT, \end{cases} \tag{3.2}$$

in which the linearized infected subsystem is naturally coupled among the different degree classes through $\Theta(t)$. Let $\mathbf{\Phi}(t)$ be the fundamental solution matrix of System (3.2) when $t \ne (m+l-1)T$ and $t \ne mT$. Then $\mathbf{\Phi}(t)$ satisfies the following form:

$$\mathbf{\Phi}(t) = \begin{bmatrix} \mathbf{\Phi_{11}}(t) & \mathbf{\Phi_{12}}(t) \\ \mathbf{0} & \mathbf{\Phi_{22}}(t) \end{bmatrix}, \tag{3.3}$$

where $\mathbf{0}$ is the n-order zero matrix, $\mathbf{\Phi_{11}}(t) = \mathrm{diag}\{e^{-\mu t}, e^{-\mu t}, \ldots, e^{-\mu t}\}$, and $\mathbf{\Phi_{22}}(t) =$

$$\mathrm{diag}\left\{e^{\int_{mT}^{mT+t}\left[\lambda(k_1)S^T_{k_1}(\tau)\frac{\omega(k_1)p(k_1)}{\langle k_i\rangle}-r-\delta\mu\right]\mathrm{d}\tau}, e^{\int_{mT}^{mT+t}\left[\lambda(k_2)S^T_{k_2}(\tau)\frac{\omega(k_2)p(k_2)}{\langle k_i\rangle}-r-\delta\mu\right]\mathrm{d}\tau}, \ldots, e^{\int_{mT}^{mT+t}\left[\lambda(k_n)S^T_{k_n}(\tau)\frac{\omega(k_n)p(k_n)}{\langle k_i\rangle}-r-\delta\mu\right]\mathrm{d}\tau}\right\}.$$

It should be noted that there is no need to give the exact form of the n-order matrix $\mathbf{\Phi_{12}}(t)$ here. In addition, columns of the matrix $\mathbf{\Phi_{22}}$ are n linearly independent particular solutions of the differential equations with respect to $(I_{k_1}, I_{k_2}, \ldots, I_{k_n})^T$.

In virtue of the Floquet theory of impulsive differential equations [29], if all eigenvalues of the monodromy matrix $\mathbf{M}$ satisfy $|\rho_i| < 1$ for all i, the disease-free periodic solution $\mathbf{E_0}(t)$ of System (3.2) is locally asymptotically stable, where

$$\begin{aligned} \mathbf{M} &= \begin{bmatrix} \mathbf{E_n}-\mathbf{Q} & \mathbf{0} \\ \mathbf{0} & \mathbf{E_n} \end{bmatrix} \mathbf{\Phi}((1-l)T) \begin{bmatrix} \mathbf{E_n} & \mathbf{0} \\ \mathbf{0} & \mathbf{E_n}-\mathbf{\Gamma} \end{bmatrix} \mathbf{\Phi}(lT)\\ &= \begin{bmatrix} (\mathbf{E_n}-\mathbf{Q})\mathbf{\Phi_{11}}(T) & * \\ \mathbf{0} & \mathbf{\Phi_{22}}((1-l)T)(\mathbf{E_n}-\mathbf{\Gamma})\mathbf{\Phi_{22}}(T) \end{bmatrix}, \end{aligned}$$

with $\mathbf{E_n}$ being the n-order identity matrix, $\mathbf{Q} = \mathrm{diag}\{q_1, q_2, \ldots, q_n\}$, and $\mathbf{\Gamma} = \mathrm{diag}\{\gamma_1, \gamma_2, \ldots, \gamma_n\}$. For the proposed model (2.2), the transmission threshold is determined by the spectral radius of the monodromy matrix, namely $\rho(\mathbf{M}) = \max\limits_{i=1,2,\ldots,2n} \rho_i$. Due to the coupling only appearing through $\Theta(t)$, the monodromy matrix $\mathbf{M}$ becomes block upper triangular in the chosen basis, thus leading to the eigenvalues being $\rho_i = (1-q_i)e^{-\mu T}$ and $\rho_{n+i} = (1-\gamma_i)e^{\int_0^T \left[\lambda(k_i)S_{k_i}^T(\tau)\frac{\omega(k_i)p(k_i)}{\langle k_i\rangle} - r - \delta\mu\right]\mathrm{d}\tau}$ for $i = 1, 2, \ldots, n$. By solving $|\rho_{n+i}| < 1$ for all $i = 1, 2, \ldots, n$, we define the following expression:

$$R_{k_i}^0 = \frac{\lambda(k_i)\omega(k_i)p(k_i)}{\langle k_i\rangle[r + \delta\mu - \frac{1}{T}\ln(1-\gamma_i)]}\Big[1 - \frac{q_i(1-e^{-\mu T})}{T\mu[1-(1-q_i)e^{-\mu T}]}\Big].$$

What needs illustration is that $\rho(\mathbf{M}) < 1$ is equivalent to $\max\limits_{i=1,2,\ldots,n} R_{k_i}^0 < 1$. If $\max\limits_{i=1,2,\ldots,n} R_{k_i}^0 < 1$ holds, then the disease-free periodic solution $\mathbf{E_0}(t)$ of System (2.2) is locally asymptotically stable. □

Lemma 3.3. *[31]. For* $\mathbf{A} = (a_{ij})_{n\times n} \in \mathbb{R}^{n\times n}$, $\lim\limits_{k\to+\infty} \mathbf{A}^k = \mathbf{0}_{n\times n}$ *if and only if* $\rho(\mathbf{A}) < 1$, *where* $\rho(\mathbf{A})$ *is the spectral radius of* $\mathbf{A}$.

Theorem 3.3. *The disease-free periodic solution* $\mathbf{E_0}(t)$ *of System (2.2) is globally attractive if* $\max\limits_{i=1,2,\ldots,n} \widehat{R_{k_i}^0} < 1$, *where* $\widehat{R_{k_i}^0} = \frac{\lambda(k_i)\omega(k_i)p(k_i)}{\langle k_i\rangle(r+\delta\mu)}\Big[1 - \frac{q_i(1-e^{-\mu T})}{T\mu[1-(1-q_i)e^{-\mu T}]}\Big]$.

Proof. From the boundedness of solutions and the positivity of parameters in System (2.2), we obtain the following:

$$\begin{cases} \dfrac{\mathrm{d}S_{k_i}(t)}{\mathrm{d}t} \le \mu - \mu S_{k_i}(t),\ t \ne mT, \\ S_{k_i}(t^+) = (1-q_i)S_{k_i}(t),\ t = mT. \end{cases} \tag{3.4}$$

Consider the following comparison system:

$$\begin{cases} \dfrac{\mathrm{d}\overline{S}_{k_i}(t)}{\mathrm{d}t} = \mu - \mu\overline{S}_{k_i}(t),\ t \ne mT, \\ \overline{S}_{k_i}(t^+) = (1-q_i)\overline{S}_{k_i}(t),\ t = mT. \end{cases} \tag{3.5}$$

It follows from Lemma 3.2 that System (3.5) has a positive periodic solution:

$$\overline{S}_{k_i}^T(t) = 1 - \frac{q_i e^{-\mu(t-mT)}}{1-(1-q_i)e^{-\mu T}},\ mT < t \le (m+1)T,$$

which is globally asymptotically stable. As a result, $\lim\limits_{t\to+\infty} \overline{S}_{k_i}(t) = \overline{S}_{k_i}^T(t) = S_{k_i}^T(t)$ holds. Based on the comparison principle of impulsive differentials equations [29], $S_{k_i}(t) \le \overline{S}_{k_i}(t)$ is further obtained. Therefore, for any $\varepsilon > 0$, there exists some $m_1 \in \mathbb{Z}^+$ such that $S_{k_i}(t) \le S_{k_i}^T(t) + \varepsilon$ for $t \in (mT, (m+1)T], m > m_1$.

On the basis of the above-mentioned result, we obtain the following when $t \in (mT, (m+1)T], m > m_1$:

$$\begin{cases} \dfrac{\mathrm{d}I_{k_i}(t)}{\mathrm{d}t} \le \lambda(k_i)\Big(S_{k_i}^T(t) + \varepsilon\Big)\Theta(t) - (r+\delta\mu)I_{k_i}(t),\ t \ne (m+l-1)T, \\ I_{k_i}(t^+) = (1-\gamma_i)I_{k_i}(t),\ t = (m+l-1)T. \end{cases} \tag{3.6}$$

Denote $\mathbf{\Phi}^{\varepsilon}_{\mathbf{22}}(t)$ as the fundamental solution matrix of the ordinary differential system as follows:

$$\frac{\mathrm{d}I_{k_i}(t)}{\mathrm{d}t} = \lambda(k_i)\Big(S^{T}_{k_i}(t) + \varepsilon\Big)\Theta(t) - (r + \delta\mu)I_{k_i}(t),\ t \neq (m + l - 1)T, i = 1, 2, \ldots, n,$$

which meets $\mathbf{\Phi}^{\varepsilon}_{\mathbf{22}}(0) = \mathbf{E_n}$. Notice that $\rho(\mathbf{\Phi}^{\varepsilon}_{\mathbf{22}}((1-l)T)(\mathbf{E_n} - \mathbf{\Gamma})\mathbf{\Phi}^{\varepsilon}_{\mathbf{22}}(lT))$ is continuous with respect to ε. Under the condition $\max\limits_{i=1,2,\ldots,n} R^0_{k_i} < 1$, the inequality $\rho(\mathbf{\Phi}^{\varepsilon}_{\mathbf{22}}((1-l)T)(\mathbf{E_n} - \mathbf{\Gamma})\mathbf{\Phi}^{\varepsilon}_{\mathbf{22}}(lT)) < 1$ still holds once ε is chosen small enough. By integrating System (3.6) from $(m + l - 1)T$ to $(m + l)T$ when $m > m_1$, we have the following:

$$\begin{aligned}\mathbf{I}(mT) \leq & \mathbf{\Phi}^{\varepsilon}_{\mathbf{22}}(mT - (m + l - 1)T)\mathbf{I}((m + l - 1)T^{+})\\ = & \mathbf{\Phi}^{\varepsilon}_{\mathbf{22}}((1 - l)T)(\mathbf{E_n} - \mathbf{\Gamma})\mathbf{I}((m + l - 1)T)\\ \leq & \mathbf{\Phi}^{\varepsilon}_{\mathbf{22}}((1 - l)T)(\mathbf{E_n} - \mathbf{\Gamma})\mathbf{\Phi}^{\varepsilon}_{\mathbf{22}}(lT)\mathbf{I}((m - 1)T).\end{aligned}$$

Then, it follows that

$$\mathbf{I}((m - 1)T) \leq \left(\mathbf{\Phi}^{\varepsilon}_{\mathbf{22}}((1 - l)T)(\mathbf{E_n} - \mathbf{\Gamma})\mathbf{\Phi}^{\varepsilon}_{\mathbf{22}}(lT)\right)^{m-m_1}\mathbf{I}((m_1 - 1)T), m > m_1.$$

When $t \in ((m - 1)T, (m + l - 1)T], m > m_1$,

$$\mathbf{I}(t) \leq \mathbf{\Phi}^{\varepsilon}_{\mathbf{22}}(t - (m - l)T)\mathbf{I}((m - 1)T). \tag{3.7}$$

Additionally, when $t \in ((m + l - 1)T, mT], m > m_1$,

$$\mathbf{I}(t) \leq \mathbf{\Phi}^{\varepsilon}_{\mathbf{22}}(t - (m + l - 1)T)(\mathbf{E_n} - \mathbf{\Gamma})\mathbf{\Phi}^{\varepsilon}_{\mathbf{22}}(lT)\mathbf{I}((m - 1)T). \tag{3.8}$$

The diagonal elements of the matrices $\mathbf{\Phi}^{\varepsilon}_{\mathbf{22}}(t - (m - l)T)$ and $\mathbf{\Phi}^{\varepsilon}_{\mathbf{22}}(t - (m + l - 1)T)(\mathbf{E_n} - \mathbf{\Gamma})\mathbf{\Phi}^{\varepsilon}_{\mathbf{22}}(lT)$ are all less than 1 if ε is restricted to be small enough and $g_{k_i}(t) < 1$ holds for $t \in (0, T], i = 1, 2, \ldots, n$, where $g_{k_i}(t) = \frac{\lambda(k_i)\omega(k_i)p(k_i)}{\langle k_i\rangle(r+\delta\mu)}\Big[1 - \frac{q_i(1-e^{-\mu t})}{\mu t[1-(1-q_i)e^{-\mu T}]}\Big]$. Hence, under the condition $\max\limits_{i=1,2,\ldots,n} \widehat{R^0_{k_i}} < 1$, we have the following:

$$\mathbf{I}(t) \leq \left(\mathbf{\Phi}^{\varepsilon}_{\mathbf{22}}((1 - l)T)(\mathbf{E_n} - \mathbf{\Gamma})\mathbf{\Phi}^{\varepsilon}_{\mathbf{22}}(lT)\right)^{m-m_1}\mathbf{I}((m_1 - 1)T), t \in ((m - 1)T, mT], m > m_1.$$

Due to $\rho(\mathbf{\Phi}^{\varepsilon}_{\mathbf{22}}((1 - l)T)(\mathbf{E_n} - \mathbf{\Gamma})\mathbf{\Phi}^{\varepsilon}_{\mathbf{22}}(lT)) < 1$, by Lemma 3.3, we have the following:

$$\lim_{t\to+\infty} \mathbf{I}(t) = \mathbf{0}_{n\times 1}.$$

Then, for any $\varepsilon > 0$, there is an integer $m_2 > m_1$ such that $I_{k_i}(t) < \varepsilon$ for $t \in (mT, (m + 1)T], m > m_2$.

For each degree class k_i, there is an inequality of the form $I_{k_i}(t) < \varepsilon$; then, by the definition $\Theta(t)$, we immediately obtain $\Theta(t) < \sum_{i=1}^{n} \omega(k_i)p(k_i)\varepsilon/\langle k_i\rangle < \sum_{i=1}^{n} k_i p(k_i)\varepsilon/\langle k_i\rangle = \varepsilon$. In addition, it's obtained from the above result that

$$\begin{cases} \dfrac{\mathrm{d}S_{k_i}(t)}{\mathrm{d}t} \geq \mu - (1 - \delta)\mu\varepsilon - \lambda(k_i)\varepsilon S_{k_i}(t) - \mu S_{k_i}(t),\ t \neq mT,\\ S_{k_i}(t^{+}) = (1 - q_i)S_{k_i}(t),\ t = mT. \end{cases} \tag{3.9}$$

Thus, construct the following comparison system:

$$\begin{cases} \dfrac{\mathrm{d}\underline{S}_{k_i}(t)}{\mathrm{d}t} = \mu - (1 - \delta)\mu\varepsilon - \lambda(k_i)\varepsilon\underline{S}_{k_i}(t) - \mu\underline{S}_{k_i}(t),\ t \neq mT,\\ \underline{S}_{k_i}(t^{+}) = (1 - q_i)\underline{S}_{k_i}(t),\ t = mT. \end{cases} \tag{3.10}$$

Utilizing Lemma 3.2, we figure out the positive periodic solution of System (3.10)

$$\underline{S}_{k_i}^T(t) = \frac{\mu-(1-\delta)\mu\varepsilon}{\lambda(k_i)\varepsilon+\mu} + \left(\underline{S}_{k_i}^* - \frac{\mu-(1-\delta)\mu\varepsilon}{\lambda(k_i)\varepsilon+\mu}\right)e^{-(\lambda(k_i)\varepsilon+\mu)(t-mT)}, mT < t \le (m+1)T, \tag{3.11}$$

where

$$\underline{S}_{k_i}^* = \frac{\mu-(1-\delta)\mu\varepsilon}{\lambda(k_i)\varepsilon+\mu}\frac{(1-q_i)(1-e^{-(\lambda(k_i)\varepsilon+\mu)T})}{1-(1-q_i)e^{-(\lambda(k_i)\varepsilon+\mu)T}}.$$

Similarly, for any $\varepsilon > 0$, there exists some integer $m_3 > m_2$ such that $S_{k_i}(t) \ge \underline{S}_{k_i}^T(t) - \varepsilon$ for $t \in (mT, (m+1)T], m > m_3$. Note that $\lim\limits_{\varepsilon\to 0}\overline{S}_{k_i}^T(t) = \lim\limits_{\varepsilon\to 0}\underline{S}_{k_i}^T(t) = S_{k_i}^T(t)$. Therefore, we have proven that $\lim\limits_{t\to+\infty} S_{k_i}(t) = S_{k_i}^T(t)$ for all i since $\underline{S}_{k_i}^T(t) - \varepsilon \le S_{k_i}(t) \le \overline{S}_{k_i}^T(t) + \varepsilon$ for sufficiently small ε. □

Corollary 3.1. *If the pulse vaccination probability satisfies $q_i > q_i^*, i = 1, 2, \ldots, n$, where q_i^* is the minimum allowable strength of vaccination defined by*

$$q_i^* = \frac{[\lambda(k_i)\omega(k_i)p(k_i) - (r+\delta\mu-\frac{1}{T}\ln(1-\gamma_i))\langle k_i\rangle]\mu T(1-e^{-\mu T})}{\lambda(k_i)\omega(k_i)p(k_i)(1-e^{-\mu T}) - [\lambda(k_i)\omega(k_i)p(k_i) - (r+\delta\mu-\frac{1}{T}\ln(1-\gamma_i))\langle k_i\rangle]\mu T e^{-\mu T}},$$

then the disease-free periodic solution $\mathbf{E_0}(t)$ of System (2.2) is globally asymptotically stable. Thus, a strong vaccination program can make infectious diseases die out ultimately with a large pulse vaccination probability.

3.3. The uniform persistence of the disease

Theorem 3.4. *If $\frac{1}{1+\alpha}\max\limits_{i=1,2,\ldots,n} R_{k_i}^0 > 1$, then there exist a positive constant $\eta > 0$ and an integer i such that for all initial values $\mathbf{x^0} = (\mathbf{S^0}, \mathbf{I^0}) \in \mathbb{R}_+^n \times \mathrm{Int}\mathbb{R}_+^n$, the solution $(\mathbf{S}(t), \mathbf{I}(t))$ of System (2.2) satisfies $I_{k_i}(t) \ge \eta$ when t is sufficiently large.*

Proof. Set

$$\Omega = \left\{ (S_{k_1}(t), S_{k_2}(t), \ldots, S_{k_n}(t), I_{k_1}(t), I_{k_2}(t), \ldots, I_{k_n}(t)) \in \mathbb{R}_+^{2n} \,\middle|\, S_{k_i}(t) + I_{k_i}(t) \le 1,\ t > 0,\ i = 1, 2, \ldots, n \right\}.$$

Define

$$\Omega_0 = \left\{ (S_{k_1}(t), S_{k_2}(t), \ldots, S_{k_n}(t), I_{k_1}(t), I_{k_2}(t), \ldots, I_{k_n}(t)) \in \Omega \,\middle|\, I_{k_i}(t) > 0,\ t > 0,\ i = 1, 2, \ldots, n \right\},$$

and $\partial\Omega_0 = \Omega_0^c = \Omega\backslash\Omega_0$. Let $P : \Omega \to \Omega$ be the Poincaré map associated with System (2.2). Namely,

$$P(\mathbf{x^0}) = (\mathbf{S}(T, \mathbf{x^0}), \mathbf{I}(T, \mathbf{x^0})), \mathbf{x^0} \in \mathbb{R}_+^{2n},$$

where $(\mathbf{S}(t, \mathbf{x^0}), \mathbf{I}(t, \mathbf{x^0}))$ is the unique solution of System (2.2) with $(\mathbf{S}(0, \mathbf{x^0}), \mathbf{I}(0, \mathbf{x^0})) = \mathbf{x^0}$. We want to prove that P is uniformly persistent with respect to $(\Omega_0, \partial\Omega_0)$.

It's available to obtain that Ω and Ω_0 are positive invariant sets. Besides, $\partial\Omega_0$ is a closed subset of Ω. Define

$$M_\partial = \left\{ \mathbf{x^0} \in \partial\Omega_0 : P^m(\mathbf{x^0}) \in \partial\Omega_0, \forall m \in \mathbb{Z}^+ \right\}.$$

We are to prove that $M_\partial = \{(\mathbf{S}, \mathbf{0}_{n\times 1}) : \mathbf{S} \geq \mathbf{0}_{n\times 1}\}$. Clearly, $\{(\mathbf{S}, \mathbf{0}_{n\times 1}) : \mathbf{S} \geq \mathbf{0}_{n\times 1}\} \subset M_\partial$. The claim $M_\partial \subset \{(\mathbf{S}, \mathbf{0}_{n\times 1}) : \mathbf{S} \geq \mathbf{0}_{n\times 1}\}$ is to be proven by way of contradiction. For an arbitrary element $\mathbf{x^0}$ of M_∂, assume that there exit $m^{'} \in \mathbb{Z}^+$ and $k_i^{'} \in \{k_1, k_2, \ldots, k_n\}$ such that $I_{k_i^{'}}(m^{'}T, \mathbf{x^0}) > 0$. Setting $I_{k_i^{'}}(m^{'}T, \mathbf{x^0})$ as the initial condition, we have $I_{k_i^{'}}\Big(t, I_{k_i^{'}}(m^{'}T, \mathbf{x^0})\Big) > 0$ for $t > m^{'}T$ based on the fact that Ω_0 is positively invariant. This result contradicts the definition of M_∂. Thus, we have $I_{k_i}(m^{'}T, \mathbf{x^0}) = 0, i = 1, 2, \ldots, n$ for any $m^{'} \in \mathbb{Z}^+$. Therefore, using Lemma 3.1 and the result obtained above, the map P has the only fixed point M_0 that satisfies $P(M_0) = M_0$ in M_∂.

Next, it's time to prove the claim that there exists $\varepsilon > 0$ such that for any initial condition $\mathbf{x^0} \in \Omega_0$, we have the following:

$$\limsup_{t\to+\infty} \max_{i\in\{1,2,\ldots,n\}} I_{k_i}(t) \geq \varepsilon. \tag{3.12}$$

If this claim is not true, then for any $\varepsilon > 0$, there exists $\mathbf{x^0}$ such that there exists t_1 satisfying $I_{k_i}(t) < \varepsilon, i = 1, 2, \ldots, n$ for $t \geq t_1$. Thus, we get the following:

$$\begin{cases} \dfrac{\mathrm{d}S_{k_i}(t)}{\mathrm{d}t} \geq \mu - (1-\delta)\mu\varepsilon - \lambda(k_i)\varepsilon S_{k_i}(t) - \mu S_{k_i}(t),\ t \neq mT, \\ S_{k_i}(t^+) = (1-q_i)S_{k_i}(t),\ t = mT. \end{cases} \tag{3.13}$$

By the comparison principle, there exists a small enough ε and an integer m_3 such that

$$S_{k_i}(t) \geq \underline{S}_{k_i}^T(t) - \varepsilon, t \geq m_3 T,$$

where $\underline{S}_{k_i}^T(t)$ is defined in (3.11). When $t \geq m_3 T$, we have the following:

$$\begin{cases} \dfrac{\mathrm{d}I_{k_i}(t)}{\mathrm{d}t} \geq \lambda(k_i)\Big(\overline{S}_{k_i}^T(t) - \varepsilon\Big)\frac{1}{1+\alpha}\Theta(t) - (r+\delta\mu)I_{k_i}(t),\ t \neq (m+l-1)T, \\ I_{k_i}(t^+) = (1-\gamma_i)I_{k_i}(t),\ t = (m+l-1)T. \end{cases} \tag{3.14}$$

By integrating the above system on $((m+l-1)T, (m+l)T], m \geq m_3 + 1$, we get the following:

$$\begin{aligned} \mathbf{I}(mT) \geq & \mathbf{\Phi}_{\mathbf{22}}^{\varepsilon}(mT - (m+l-1)T)\mathbf{I}((m+l-1)T^+) \\ = & \mathbf{\Phi}_{\mathbf{22}}^{\varepsilon}((1-l)T)(\mathbf{E_n} - \mathbf{\Gamma})\mathbf{\Phi}_{\mathbf{22}}^{\varepsilon}(lT)\mathbf{I}((m-1)T), \end{aligned}$$

where $\mathbf{\Phi}_{\mathbf{22}}^{\varepsilon}$ is the fundamental solution matrix with $\mathbf{\Phi}_{\mathbf{22}}^{\varepsilon}(0) = \mathbf{E_n}$ of the following linear ordinary differential system:

$$\frac{\mathrm{d}I_{k_i}(t)}{\mathrm{d}t} = \lambda(k_i)\Big(\overline{S}_{k_i}^T(t) - \varepsilon\Big)\frac{1}{1+\alpha}\Theta(t) - (r+\delta\mu)I_{k_i}(t), i = 1, 2, \ldots, n.$$

Then,

$$\mathbf{I}(t) \geq \left[\mathbf{\Phi}_{\mathbf{22}}^{\varepsilon}(mT - (m+l-1)T)(\mathbf{E_n} - \mathbf{\Gamma})\mathbf{\Phi}_{\mathbf{22}}^{\varepsilon}(lT)\right]^{m-m_1}\mathbf{I}((m_1-1)T), t \in ((m-1)T, mT], m \geq m_3.$$

Under the condition $\frac{1}{1+\alpha}\max_{i=1,2,\ldots,n} R_{k_i}^0 > 1$, we can deduce $I_{k_i}(t) \to +\infty$ as $t \to +\infty$ for sufficiently small ε, which contradicts the boundedness of $I_{k_i}(t)$ in System (2.2). Therefore, the above claim can be proven through the method of contradiction.

According to the above claims, it follows that M_0 is an isolated invariant set for P in Ω, and $W^s(M_0)\cap\Omega_0=\emptyset$, where $W^s(M_0)$ is the stable set of M_0 for P. Note that $\omega(\mathbf{x^0})=M_0$ for any $\mathbf{x^0}\in M_\partial$, and M_0 can't form a cycle in $\partial\Omega_0$. By the acyclicity theorem on the uniform persistence for maps in [32], it can be proven that P is uniformly persistent with respect to $(\Omega_0,\partial\Omega_0)$. As a result, there exist a large enough $\overline{m}\in\mathbb{Z}^+$ and a small enough $\varepsilon>0$ such that

$$P^m(\mathbf{x^0})=(\mathbf{S}(mT^+),\mathbf{I}(mT^+))>\varepsilon(\mathbf{1}_{n\times1},\mathbf{1}_{n\times1}),m>\overline{m}.$$

Notice that

$$\frac{\mathrm{d}I_{k_i}(t)}{\mathrm{d}t}\geq-(r+\delta\mu)I_{k_i}(t),\ t\neq(m+l-1)T.$$

For $t\in((m+l-1)T,(m+l)T],m>\overline{m}+1$, we have the following:

$$\begin{aligned}I_{k_i}(t)&\geq e^{-(r+\delta\mu)(t-(m+l-1)T)}I_{k_i}((m+l-1)T^+)\\&=e^{-(r+\delta\mu)(t-(m+l-1)T)}(1-\gamma_i)I_{k_i}((m+l-1)T)\\&\geq e^{-(r+\delta\mu)(t-(m+l-1)T)}(1-\gamma_i)e^{-(r+\delta\mu)lT}I_{k_i}((m-1)T^+)\\&\geq e^{-(r+\delta\mu)(t-(m-1)T)}(1-\gamma_i)\varepsilon\triangleq\eta.\end{aligned}$$

□

Theorem 3.5. *If* $\frac{1}{1+\alpha}\max\limits_{i=1,2,\ldots,n}R^0_{k_i}>1$*, then System (2.2) is uniformly persistent.*

Proof. It follows from Lemma 3.1 that

$$\begin{cases}\dfrac{\mathrm{d}S_{k_i}(t)}{\mathrm{d}t}\geq\mu-(1-\delta)\mu-\lambda(k_i)S_{k_i}(t)-\mu S_{k_i}(t),\ t\neq mT,\\ S_{k_i}(t^+)=(1-q_i)S_{k_i}(t),\ t=mT.\end{cases}\tag{3.15}$$

We construct the following auxiliary system:

$$\begin{cases}\dfrac{\mathrm{d}\underline{S}^{'}_{k_i}(t)}{\mathrm{d}t}=\mu-(1-\delta)\mu-\lambda(k_i)\underline{S}^{'}_{k_i}(t)-\mu\underline{S}^{'}_{k_i}(t),\ t\neq mT,\\ \underline{S}^{'}_{k_i}(t^+)=(1-q_i)\underline{S}^{'}_{k_i}(t),\ t=mT.\end{cases}\tag{3.16}$$

By Lemma 3.2, the positive periodic solution of System (3.16) is as follows:

$$\underline{S}^{'T}_{k_i}(t)=\frac{\mu-(1-\delta)\mu}{\lambda(k_i)+\mu}+\left(\underline{S}^{'*}_{k_i}(t)-\frac{\mu-(1-\delta)\mu}{\lambda(k_i)+\mu}\right)e^{-(\lambda(k_i)+\mu)(t-mT)},mT<t\leq(m+1)T,$$

where

$$\underline{S}^{'*}_{k_i}(t)=\frac{\mu-(1-\delta)\mu}{\lambda(k_i)+\mu}\frac{(1-q_i)(1-e^{-(\lambda(k_i)+\mu)T})}{1-(1-q_i)e^{-(\lambda(k_i)+\mu)T}}.$$

In accordance with the comparison principle, we have $S_{k_i}(t)\geq\underline{S}^{'}_{k_i}(t)$. Note that $\lim\limits_{t\to+\infty}\underline{S}^{'}_{k_i}(t)=\underline{S}^{'T}_{k_i}(t)$. Hence, for any $\varepsilon>0$, there exists some $m_0\in\mathbb{Z}^+$ such that $S_{k_i}(t)\geq\underline{S}^{'T}_{k_i}(t)-\varepsilon$ when $t\in(mT,(m+1)T],m>m_0$. Consequently, it's proven that there must be a positive constant ζ_i such that $S_{k_i}(t)\geq\zeta_i$ for a large enough t, where $\zeta_i=\underline{S}^{'T}_{k_i}(t)-\varepsilon>0$.

By Lemma 3.1 and Theorem 3.4, there exists i such that $\Theta(t) \geq \frac{\omega(k_i)p(k_i)\eta}{\langle k_i\rangle} \geq \min_{i\in N}\{\omega(k_i)p(k_i)\}\frac{\eta}{\langle k_i\rangle}$ for t sufficiently large. For any integer $j \neq i$, we obtain the following:

$$\frac{\mathrm{d}I_{k_j}(t)}{\mathrm{d}t} \geq \lambda(k_j)\zeta_j \frac{\min_{i\in N}\{\omega(k_i)p(k_i)\}\eta}{\langle k_i\rangle + \alpha \min_{i\in N}\{\omega(k_i)p(k_i)\}\eta} - (r+\delta\mu)I_{k_j}(t).$$

Then, the comparison system is constructed as follows:

$$\begin{cases} \dfrac{\mathrm{d}U_{k_j}(t)}{\mathrm{d}t} = \lambda(k_j)\zeta_j \dfrac{\min_{i\in N}\{\omega(k_i)p(k_i)\}\eta}{\langle k_i\rangle + \alpha \min_{i\in N}\{\omega(k_i)p(k_i)\}\eta} - (r+\delta\mu)U_{k_j}(t),\ t \neq (m+l-1)T, \\ U_{k_j}(t^+) = (1-\gamma_i)U_{k_j}(t),\ t = (m+l-1)T. \end{cases} \tag{3.17}$$

Utilizing Lemma 3.2, we have the positive periodic solution of System (3.17) satisfying

$$U_{k_j}^T(t) = \frac{\varpi_j}{r+\delta\mu} + \left(U_{k_j}^* - \frac{\varpi_j}{r+\delta\mu}\right)e^{-(r+\delta\mu)(t-(m+l-1)T)},\ (m+l-1)T < t \leq (m+l)T,$$

where

$$\varpi_j = \lambda(k_j)\zeta_j \frac{\min_{i\in N}\{\omega(k_i)p(k_i)\}\eta}{\langle k_i\rangle + \alpha \min_{i\in N}\{\omega(k_i)p(k_i)\}\eta},$$

and

$$U_{k_j}^* = \frac{\varpi_j}{r+\delta\mu}\frac{(1-\gamma_i)(1-e^{-(r+\delta\mu)T})}{1-(1-\gamma_i)e^{-(r+\delta\mu)T}},$$

which is globally asymptotically stable. Similarly, for any $\varepsilon > 0$ and t sufficiently large, we get the following:

$$I_{k_j}(t) \geq U_{k_j}^T(t) - \varepsilon \triangleq \varsigma_j > 0.$$

Hence, we have proven that all solutions of System (2.2) eventually enter in the following region:

$$\underline{\Omega} = \left\{ \left\{(S_{k_i}(t), I_{k_i}(t))\right\}_{i=1}^n \in \mathbb{R}_+^{2n} \,\middle|\, \zeta_i \leq S_{k_i}(t) \leq 1, \max\{\eta, \varsigma_i\} \leq I_{k_i}(t) \leq 1,\ t > 0,\ i = 1,2,\ldots,n \right\},$$

where ζ_i and $\max\{\eta, \varsigma_i\}$ are independent of the given initial condition of System (2.2). □

Corollary 3.2. *Define the minimum allowable strength of cure as follows:*

$$\gamma_i^* = 1 - e^{T\left\{r+\delta\mu - \frac{\lambda(k_i)\omega(k_i)p(k_i)}{(1+\alpha)\langle k_i\rangle}\left[1 - \frac{q_i(1-e^{-\mu T})}{T\mu[1-(1-q_i)e^{-\mu T}]}\right]\right\}}.$$

If the pulse cure rate satisfies $\gamma_i < \gamma_i^*, i = 1,2,\ldots,n$, then System (2.2) is uniformly persistent. This implies that the disease persists in the population when the screening rate is low.

4. Numerical simulations

In this section, we present some numerical simulations to examine the impact of parameter values on the disease dynamics, visualize some of our theoretical results, and investigate the effects of double impulsive controls quantitatively. The numerical simulations in this study are performed by directly integrating the deterministic degree-based mean-field ordinary differential equations derived in Section 2, that is, while the model is motivated by network epidemiology, the simulations are deterministic and based on the same system used for the theoretical analysis. Thus, the numerical results serve as a direct validation of the analytical findings. For practical convenience, suppose k_i to be i, which ranges from 1 to n. The maximum degree of nodes is assumed to be $k_n = n = 100$. For the underlying topology, we consider the transmission of disease based on the scale-free network with the degree distribution $p(k_i) = \varrho k_i^{-3}$, where $\varrho = 0.8319$ makes $\sum_{i=1}^{100} p(k_i) = 1$ hold. By calculation, the average degree of the network is $\langle k_i \rangle = 1.3602$. Moreover, the propagation probability is taken as $\lambda(k_i) = \lambda_0 \frac{k_i}{1+k_i}$, where λ_0 is the basal transmission rate. For each node, choose $\omega(k_i) = \frac{k_i^{0.5}}{1+k_i^{0.5}}$ to characterize the saturated infectivity of the node with degree k_i. It is necessary to clearly state that the periodic oscillations observed in the following figures do not result from the continuous network-based SIR epidemic model. Instead, they are directly imposed by the periodic impulsive controls. Thus, the periodic solutions depicted in this section are forced by the periodic impulsive intervention strategy.

4.1. Impact of model parameters on the transmission thresholds

As a crucial criterion, the transmission thresholds $R^0_{k_i}$ play a key role in determining the transmission dynamics of disease across the network. In this subsection, we examine the influence of model parameters on controlling the transmission of disease. Following [33, 34], we adopt the analytical expression $\Upsilon_\chi^{R^0_{k_i}} = \frac{\partial R^0_{k_i}}{\partial \chi} \times \frac{\chi}{R^0_{k_i}}$ to measure the relative change of the transmission threshold $R^0_{k_i}$ which results from a change in a specific parameter, where χ is any parameter involved in Model (2.2). By calculating partial derivatives of the threshold with respect to all relevant parameters, for $i = 1, 2, \ldots, n$, we obtain

$$\frac{\partial R^0_{k_i}}{\partial \delta} < 0, \frac{\partial R^0_{k_i}}{\partial \lambda_0} > 0, \frac{\partial R^0_{k_i}}{\partial r} < 0, \frac{\partial R^0_{k_i}}{\partial q_i} < 0, \frac{\partial R^0_{k_i}}{\partial \gamma_i} < 0, \frac{\partial R^0_{k_i}}{\partial T} > 0$$

when model parameters are in the following region Ξ defined by

$$\left\{ (\mu, \delta, \lambda_0, r, q_i, \gamma_i, T) \in \mathbb{R}^7_+ \;\middle|\; \max\left\{ \frac{q_i(1-e^{-\mu T})}{T\mu[1-(1-q_i)e^{-\mu T}]}, \frac{T\mu}{1-e^{-\mu T}}, [q_i(T\mu-1)+2]e^{-\mu T} \right\} < 1 \right\}.$$

From these inequalities, it is found that the parameters δ, r, q_i, and γ_i are negatively correlated with the threshold $R^0_{k_i}$ for all i. On the other hand, both the basal transmission rate λ_0 and the pulse vaccination period T are positively correlated with the threshold $R^0_{k_i}$. Take the parameters $\mu = 0.15, \delta = 0.1, \lambda_0 = 0.7, r = 0.02, q_1 = 0.2, \gamma_1 = 0.1, T = 2$ with $i = 1$ as an example. It can be observed from Figure 1(a) that the transmission threshold $R^0_{k_1}$ consistently increases with the natural birth (death) rate μ when the vertical transmission rate $1 - \delta$ is large. However, for a small $1 - \delta$, the threshold $R^0_{k_i}$ initially increases and then decreases as μ increases. This intriguing result highlights the significant impact of vertical

transmission on the spread of disease when mother-infant transmission dominates, and the vaccine has not yet interrupted the infection.

To quantitatively assess the influence of key parameters on the transmission threshold $R^0_{k_i}$, we perform a global sensitivity analysis using the Partial Rank Correlation Coefficient (PRCC) method. The uncertain parameters considered are as follows: the birth/death rate $\mu \in (0, 1)$, the vertical transmission factor $\delta \in (0, 1)$ with $1 - \delta$ being the vertical infection rate, the transmission rate $\lambda_0 > 0$, the saturation coefficient $\alpha > 0$, the recovery rate $r \in (0, 1)$, the pulse period $T > 0$, the pulse vaccination rate $q_i \in (0, 1)$, and the pulse cure rate $r_i \in (0, 1)$. A Latin hypercube sample of size 1000 is drawn from uniform distributions over the specified ranges, and PRCC values are computed for a representative degree class $k_i = 80$. All 1000 samples yield valid $R^0_{k_i}$ values. The results are shown in Figure 1(b). The most influential parameter is the transmission rate λ_0 (PRCC = +0.869, $P < 0.001$), thus indicating that reducing λ_0 has the strongest effect in lowering the threshold $R^0_{k_i}$. The recovery rate r (PRCC = −0.665) and the vertical transmission factor δ (PRCC = −0.405) also exhibit strong negative correlations, meaning that a faster recovery or reduced vertical transmission significantly decreases $R^0_{k_i}$. The pulse period T shows a substantial positive correlation (PRCC = +0.507), confirming that more frequent impulsive interventions are beneficial. The pulse vaccination rate q_i and cure rate γ_i have weaker negative correlations (PRCC = −0.317 and −0.275, respectively), while the birth/death rate μ exhibits a very weak negative effect (PRCC = −0.074, p = 0.0195) that is still statistically significant. All p-values are below 0.05, thus confirming the statistical significance of these correlations. These findings provide quantitative guidance for disease control: priority should be given to reducing transmission, enhancing recovery, and increasing the intervention frequency, whereas solely raising the pulse vaccination or cure coverage yields comparatively smaller benefits.

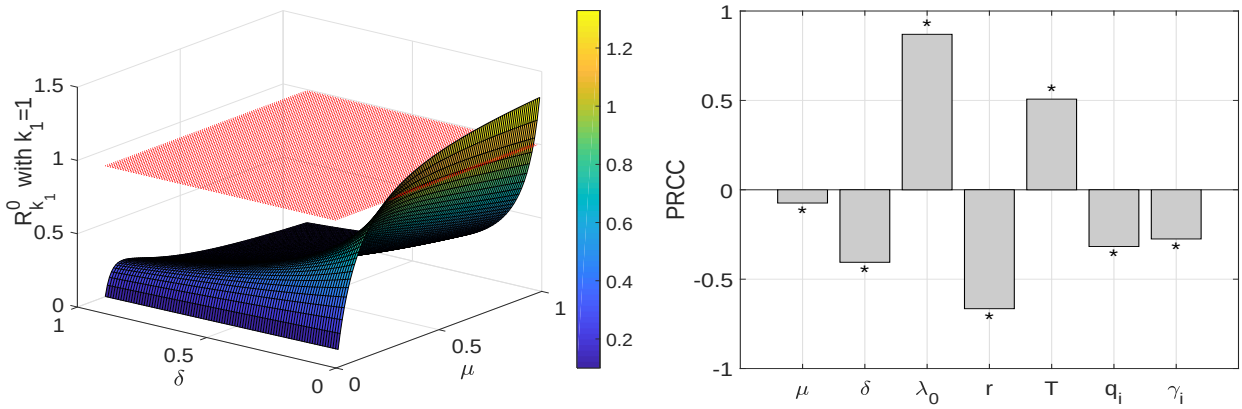

(a) (b)

Figure 1. The joint impact of μ and δ on the transmission threshold $R^0_{k_1}$ [panel (a)] and PRCC for transmission threshold [panel (b)].

4.2. Dynamical behaviors of epidemic model in different cases

In this subsection, we perform simulations for System (2.2) to observe the evolution of a disease under different conditions. The model parameters are set as $\mu = 0.15, \delta = 0.65, \lambda_0 = 5, r = 0.05, \alpha = 0.002, q_i = 0.8, \gamma_i = 0.01, T = 2$, and $l = 0.3$. For each degree class, choose the initial condition

$S_{i,0} = 0.6, I_{i,0} = 0.3$. Accordingly, the transmission threshold is calculated as $\max\limits_{i=1,2,\ldots,n} \widehat{R^0_{k_i}} = 0.6844 < 1$. Without loss of generality, we examine the evolution of nodes with degree $k_i = 80$ as an example. Figure 2 illustrates that $S_{80}(t)$ converges to a positive periodic solution, while $I_{80}(t)$ approaches zero as t becomes sufficiently large. This indicates that the disease eventually becomes extinct over time, thus validating the statements in Theorem 3.3. Furthermore, from Corollary 3.1, we know that the disease-free periodic solution $\mathbf{E_0}(t)$ of System (2.2) is globally asymptotically stable, a conclusion supported by several numerical experiments with different initial conditions.

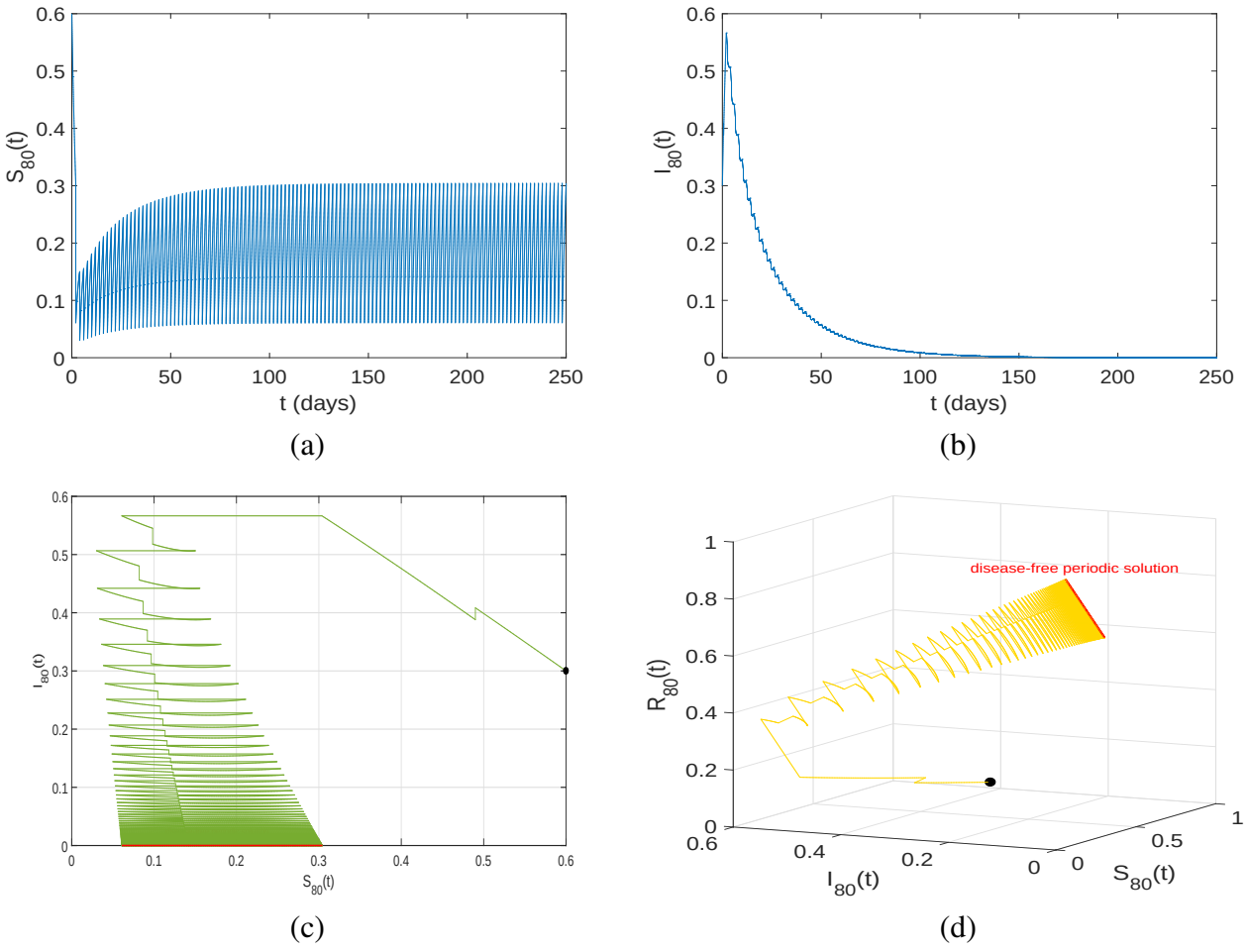

Figure 2. When $\max\limits_{i=1,2,\ldots,n} \widehat{R^0_{k_i}} < 1$, the dynamical behavior of System (2.1) with the initial condition $S_{i,0} = 0.6, I_{i,0} = 0.3$ for all i. (a) Time series of $S_{80}(t)$. (b) Time series of $I_{80}(t)$. (c) Phase portrait of $S_{80}(t)$ and $I_{80}(t)$. (d) Phase portrait of $S_{80}(t)$, $I_{80}(t)$, and $R_{80}(t)$.

Set the model parameters as $\mu = 0.15, \delta = 0.07, \lambda_0 = 0.98, r = 0.005, \alpha = 0.002, q_i = 0.3, \gamma_i = 0.1, T = 2$, and $l = 0.3$ and the initial condition as $S_{i,0} = 0.5, I_{i,0} = 0.35$ for all i. By calculation, $\frac{1}{1+\alpha} \max\limits_{i=1,2,\ldots,n} R^0_{k_i} = 1.0126 > 1$. According to Figure 3, System (2.2) exhibits an endemic periodic solution, oscillating distinctly due to the introduction of double impulsive strategies. The numerical results in Figure 3 further show that $I_{80}(t)$ remains strictly positive over time, thus confirming the persistence of disease in the network as stated in Theorem 3.4.

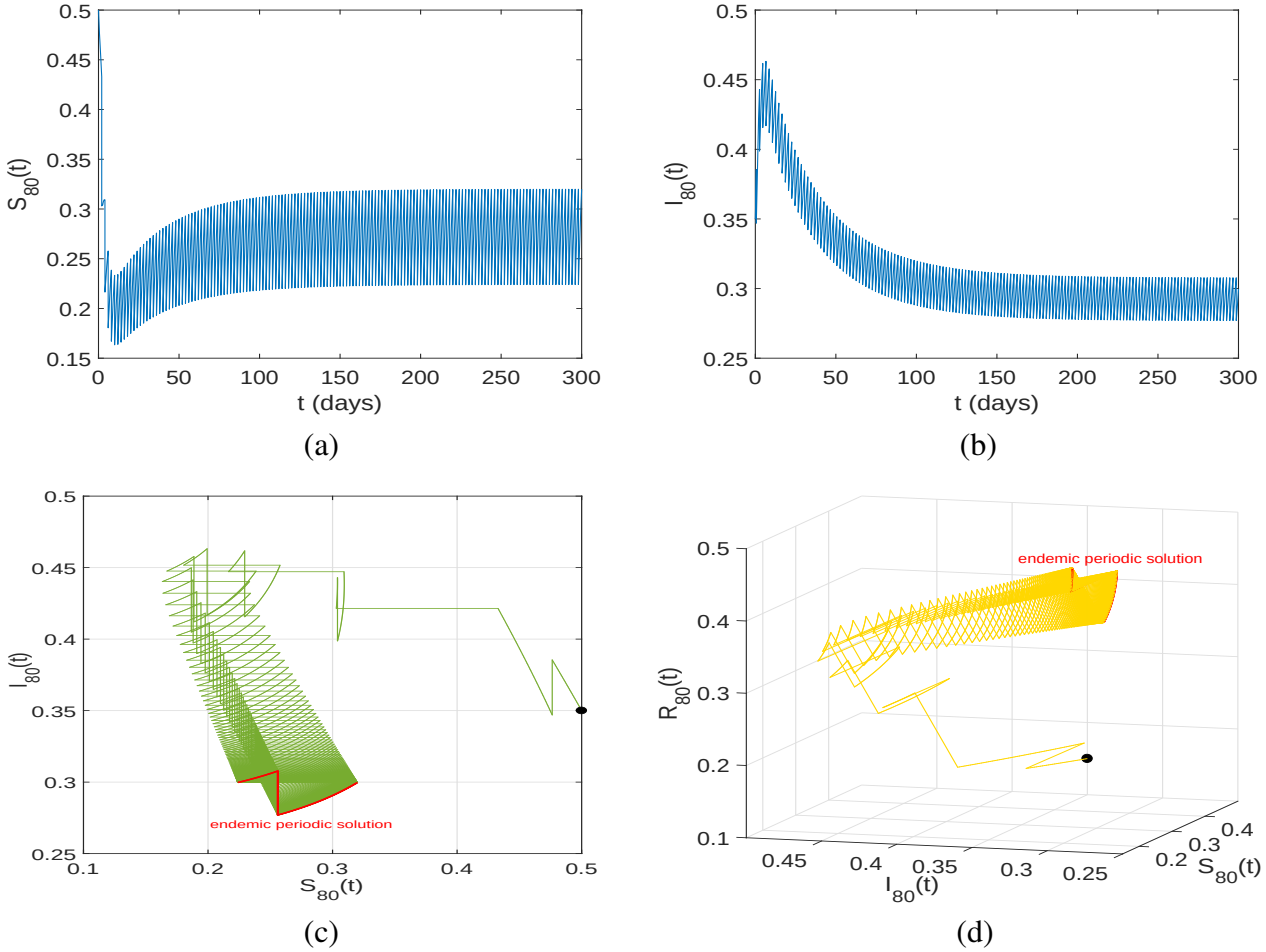

Figure 3. When $\frac{1}{1+\alpha}\max_{i=1,2,\ldots,n} R^0_{k_i} > 1$, the dynamical behavior of System (2.1) with the initial condition $S_{i,0} = 0.5, I_{i,0} = 0.35$ for all i. (a) Time series of $S_{80}(t)$. (b) Time series of $I_{80}(t)$. (c) Phase portrait of $S_{80}(t)$ and $I_{80}(t)$. (d) Phase portrait of $S_{80}(t)$, $I_{80}(t)$, and $R_{80}(t)$.

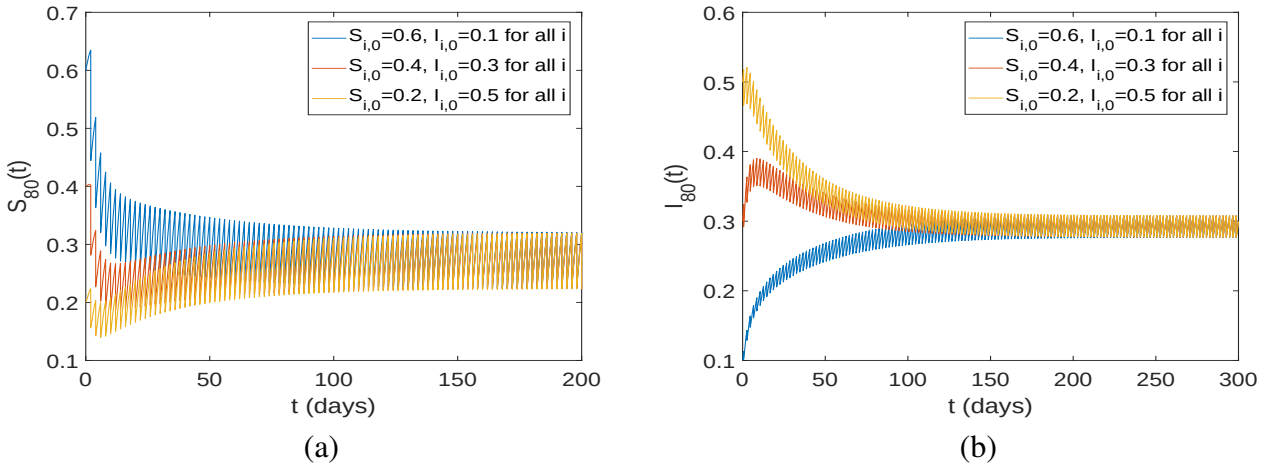

Figure 4. Time series of $S_{80}(t)$ and $I_{80}(t)$ with three sets of initial conditions.

To assess the impact of initial conditions on the disease dynamics, we consider three different sets of initial values, as shown in the legend of Figure 4. Examining nodes with degree $k_i = 80$ as an example, we observe that both $S_{80}(t)$ and $I_{80}(t)$ converge to the same positive periodic solutions, regardless of the initial conditions. This result demonstrates that the disease remains uniformly persistent under the given conditions, thus validating Theorem 3.5.

4.3. Effects of double impulsive controls on the transmission of disease

To examine the relationship between the transmission threshold $R^0_{k_i}$ and the pulse period T, pulse vaccination probability q_i, or pulse cure rate γ_i, we set the parameters as $\mu = 0.15, \delta = 0.85, \lambda_0 = 0.98, r = 0.01$, and either $\gamma_i = 0.05$ or $q_i = 0.05$, respectively. Under these parameter settings, Figure 5(a),(b) illustrate the combined effect of T, q_i, and γ_i on $R^0_{k_i}$. The results indicate that $R^0_{k_i}$ is positively correlated with T, while it is negatively correlated with q_i and γ_i. By comparing these two plots in Figure 5, we find that when both rates are extremely low, a given value of q_i results in a lower $R^0_{k_i}$ than the same value of γ_i. However, above a small critical value, γ_i becomes more effective in reducing $R^0_{k_i}$ than q_i. That suggests that, provided there are sufficient medical resources, increasing the pulse screening with the treatment rate is more effective in accelerating the eradication of disease.

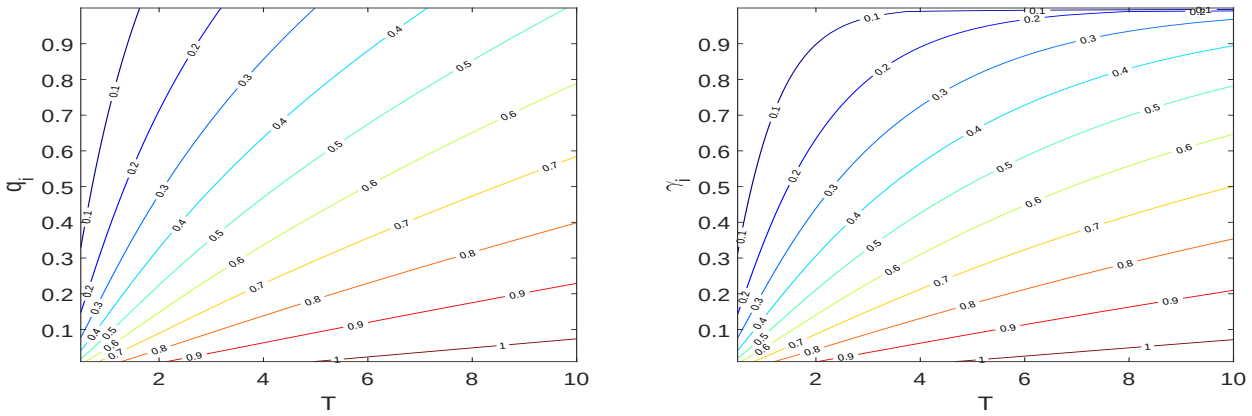

(a) (b)

Figure 5. Contour plot of the threshold $R^0_{k_i}$ for pulse period T, pulse vaccination probability q_i [panel (a)], and pulse cure rate γ_i [panel (b)].

To investigate the impact of the pulse period T on the transmission dynamics of disease, we simulate the epidemic model (2.2) with various pulse periods $T = 1, 3, 5$, while keeping the remaining parameters fixed at $\mu = 0.15, \delta = 0.09, \lambda_0 = 0.95, r = 0.05, \alpha = 0.02, q_i = 0.3, \gamma_i = 0.1$, and $l = 0.3$. Besides, the initial condition is set as $S_{i,0} = 0.6, I_{i,0} = 0.1$ for all i. Taking nodes with degree $k_i = 80$ as an example, Figure 6 shows that as T increases, the oscillation frequency of $S_{80}(t)$ or $I_{80}(t)$ decreases. Additionally, there is a positive correlation between the infected population size and the pulse period once the system reaches a stable periodic solution. Notably, the disease is eliminated when vaccinations and screenings with treatments are administered frequently enough to meet a specified threshold. Additionally, the results indicate that the more frequently the pulse interventions are applied, the faster the disease is eradicated. Therefore, as long as medical resources allow, increasing the frequency of vaccination and screening with treatment proves to be an effective strategy to control epidemic out-

breaks.

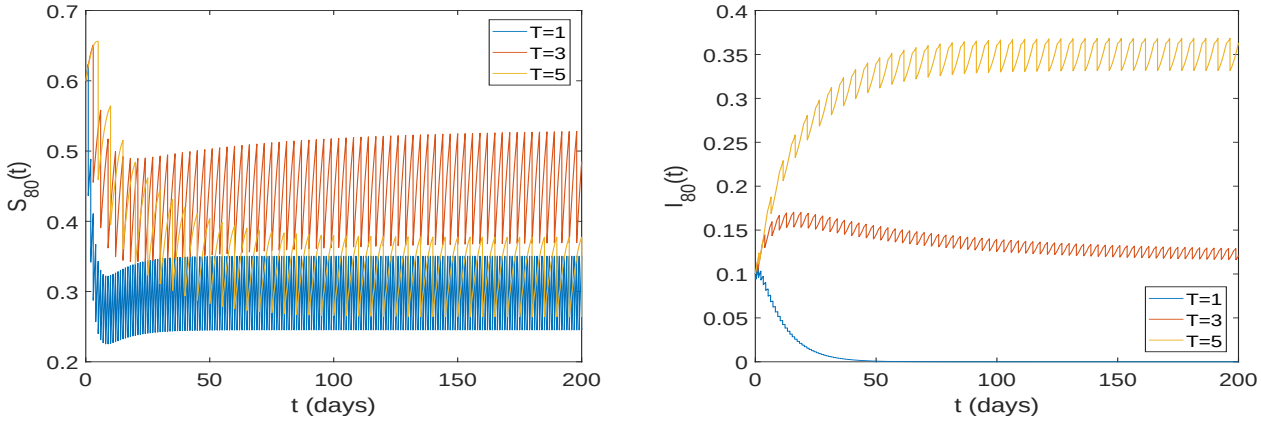

Figure 6. Time series of $S_{80}(t)$ and $I_{80}(t)$ with the initial condition $S_{i,0} = 0.6, I_{i,0} = 0.1$ for all i.

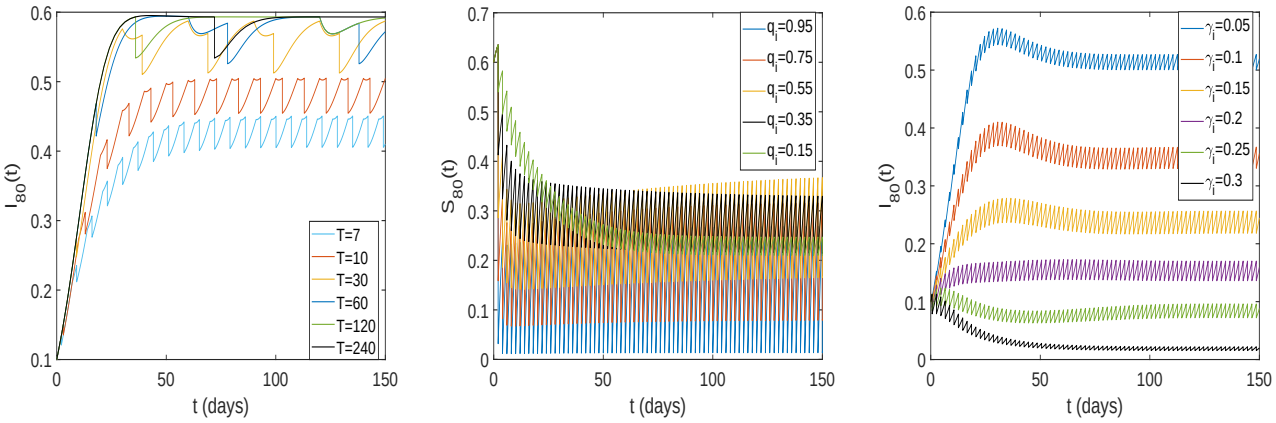

Figure 7. Time series of $S_{80}(t)$ and $I_{80}(t)$ with the initial condition $S_{i,0} = 0.6, I_{i,0} = 0.1$ for all i.

To further investigate the effects of impulsive control parameters on the oscillation amplitude, we vary the pulse period T, pulse vaccination rate q_i, and pulse cure rate γ_i. The initial conditions are set as $S_{i,0} = 0.6, I_{i,0} = 0.1$ for all degree classes. For illustration, we focus on nodes with degree $k_i = 80$, namely $S_{80}(t)$ and $I_{80}(t)$. When studying the effect of the pulse period T on the amplitude, we choose $T = 7, 10, 30, 60, 120$, and 240 while keeping the other parameters fixed as $\mu = 0.15, \delta = 0.09, \lambda_0 = 0.95, r = 0.05, \alpha = 0.02, q_i = 0.3, \gamma_i = 0.1$, and $l = 0.3$. As shown in Figure 7(a), when T increases from small to moderate values, the amplitude of $I_{80}(t)$ first increases. This is because a longer inter-pulse interval allows more time for disease transmission, thus leading to a higher peak. However, when T exceeds a certain threshold, the amplitude begins to decrease and eventually reaches a saturation. This non-monotonic behavior arises from the saturated incidence and the depletion of

susceptible individuals: for very long periods, the infection peak is limited by the saturated contact rate, while the natural recovery and death processes reduce the trough, thus narrowing the amplitude. The oscillation frequency monotonically with decreases T. When studying the effect of the pulse vaccination rate q_i on the amplitude, we choose $q_i = 0.15, 0.35, 0.55, 0.75$, and 0.95 while keeping the other parameters fixed as $\mu = 0.15, \delta = 0.09, \lambda_0 = 0.95, r = 0.05, \alpha = 0.02, T = 2, \gamma_i = 0$, and $l = 0.3$. Since pulse vaccinations directly reduce the susceptible population, we examine $S_{80}(t)$ in Figure 7(b), which shows that increasing q_i leads to a larger amplitude of $S_{80}(t)$. A higher vaccination coverage removes more susceptible individuals at each pulse, thus causing deeper troughs. When studying the effect of the pulse cure rate γ_i on the amplitude, we choose $\gamma_i = 0.05, 0.1, 0.15, 0.2, 0.25$, and 0.3 while keeping the other parameters fixed as $\mu = 0.05, \delta = 0.09, \lambda_0 = 0.98, r = 0.01, \alpha = 0.02, T = 2, q_i = 0$, and $l = 0.3$. Pulse treatment acts on infected individuals, so we present $I_{80}(t)$. Figure 7(c) reveals that as γ_i increases, the amplitude of $I_{80}(t)$ initially rises and then falls. For a small γ_i, the treatment is weak; increasing it reduces the post-pulse infected trough, thus widening the amplitude. However, beyond a critical γ_i, treatment becomes so effective that the infection is suppressed before reaching a high peak, and the amplitude declines. This indicates an optimal treatment intensity that maximises the oscillatory response, beyond which the system approaches the no-infection regime.

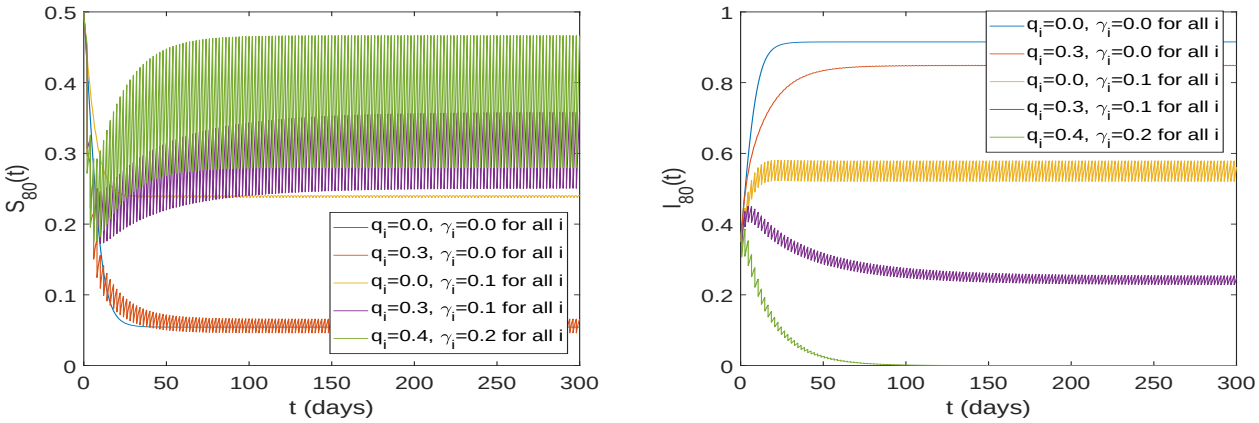

(a) (b)

Figure 8. Time series of $S_{80}(t)$ and $I_{80}(t)$ with the initial condition $S_{i,0} = 0.5, I_{i,0} = 0.35$ for all i.

To evaluate the effectiveness of dual impulsive controls, comparison experiments are conducted using the epidemic model (2.2), with five typical scenarios with different combinations of pulse vaccination and cure rates: $(q_i, \gamma_i) = (0, 0), (0.3, 0), (0, 0.1), (0.3, 0.1)$, and $(0.4, 0.2)$ for all i. The reminding parameters are set as $\mu = 0.15, \delta = 0.09, \lambda_0 = 0.95, r = 0.005, \alpha = 0.02, T = 2, l = 0.3$ and the initial condition is chosen as $S_{i,0} = 0.5, I_{i,0} = 0.35$ for all i. Take nodes with degree $k_i = 80$ as an example, Figure 8 exhibits that in the absence of pulse interventions, the time series of $S_{80}(t)$ and $I_{80}(t)$ remain smooth without oscillations. Compared to the uncontrolled scenario, implementing a single pulse control method reduces the final infected population size. However, a significant reduction in prevalence is only achieved when both impulsive controls are applied together. Furthermore, increasing the intensity of both pulse vaccinations and screenings with treatments can lead to the complete eradication of the disease. These findings highlight that effective control requires an integrated approach combin-

ing vaccination and medical treatment. For comprehensive disease prevention and management, both strategies should be considered to effectively curb disease transmission .

5. Conclusions and discussion

In this work, we developed an SIR epidemic model on complex networks, thereby incorporating vertical transmission, saturated incidence, pulse vaccination, and screening with treatment. We analyzed the model's dynamical properties both theoretically and numerically, thus providing insights that can guide the control and prevention of infectious diseases through multiple pulse interventions. The key findings of this study are summarized as follows.

First, the positively invariant set $\overline{\Omega}$ for System (2.1) was identified. To assess disease transmission, two critical thresholds, $R^0_{k_i}$ and $\widehat{R^0_{k_i}}$, were introduced and defined, which determine the progression of disease. It was obtained that System (2.2) admits a disease-free periodic solution $\mathbf{E_0}(t)$. Using the Floquet theorem, the disease-free periodic solution $\mathbf{E_0}(t)$ was proven to be locally asymptotically stable when $\max\limits_{i=1,2,\ldots,n} R^0_{k_i} < 1$. Furthermore, by applying the comparison principle for impulsive differential equations, the global attractivity of $\mathbf{E_0}(t)$ was demonstrated when $\max\limits_{i=1,2,\ldots,n} \widehat{R^0_{k_i}} < 1$. Additionally, by utilizing the uniform persistence of the Poincaré map, we derived a sufficient condition for the persistence of disease: if $\frac{1}{1+\alpha} \max\limits_{i=1,2,\ldots,n} R^0_{k_i} > 1$, then System (2.2) exhibits a uniform persistence, thus leading to the establishment of an endemic state. Regarding double impulsive controls, the minimum required strengths of vaccinations and screenings with treatments are defined in Corollaries 3.1 and 3.2, respectively, providing necessary conditions to implement effective impulsive strategies to eliminate the disease.

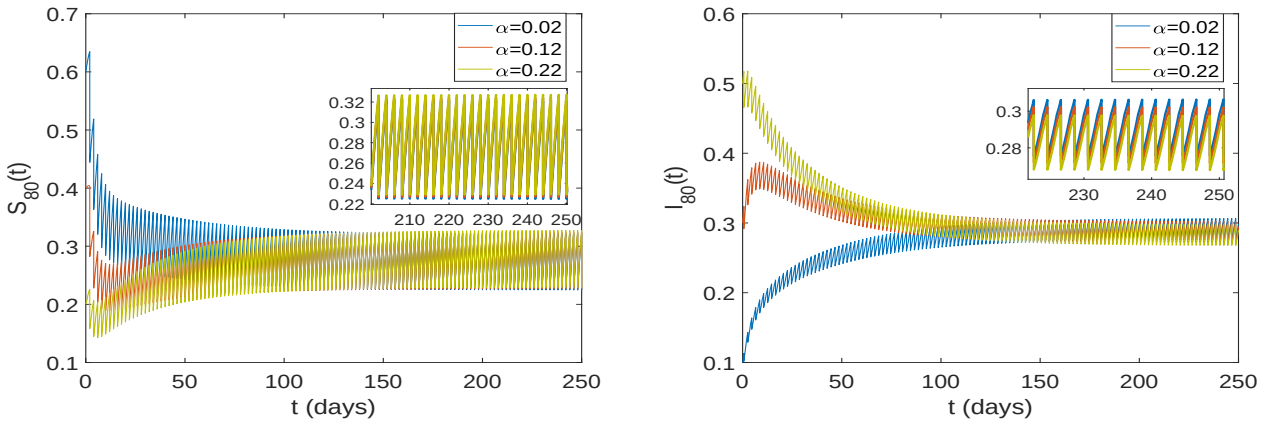

Figure 9. Time series of $S_{80}(t)$ and $I_{80}(t)$ with parameters $\mu = 0.15, \delta = 0.07, \lambda_0 = 0.98, r = 0.005, q_i = 0.3, \gamma_i = 0.1, T = 2, l = 0.3$ and different α shown in the legend, corresponding to $\max\limits_{i=1,2,\ldots,n} R^0_{k_i} = 1.0146$, and $\frac{1}{1+\alpha} \max\limits_{i=1,2,\ldots,n} R^0_{k_i} = 0.9947, 0.9059$, and 0.8316, respectively. Initial conditions $(S_{i,0}, I_{i,0})$ are set as $(0.6, 0.1)$, $(0.4, 0.3)$, and $(0.2, 0.5)$ for the three scenarios, respectively.

In addition, numerical simulations and analysis for Model (2.2) were performed. While the dynam-

ics of System (2.2) are well understood for the cases where $\max_{i=1,2,\ldots,n} R^0_{k_i} < 1$ and $\frac{1}{1+\alpha} \max_{i=1,2,\ldots,n} R^0_{k_i} > 1$, further investigation is needed when the threshold indicator $\max_{i=1,2,\ldots,n} R^0_{k_i}$ falls within the range $(1, 1+\alpha)$. Based on the numerical results shown in Figure 9, we propose a conjecture that the endemic periodic solution is globally asymptotically stable in this intermediate range. This is supported by time series simulations of $S_{80}(t)$ and $I_{80}(t)$ under three different parameter sets that satisfy $1 < \max_{i=1,2,\ldots,n} R^0_{k_i} < 1+\alpha$.

Compared to the scenario without impulsive control, the application of either pulse vaccination or treatment significantly reduces the density of infected individuals. Furthermore, the results indicate that the combined implementation of both pulse interventions is more effective than using a single measure alone. From a public health perspective, an integrated approach that includes both vaccinations and screenings with treatments are not only more effective but also practically viable to eradicate the disease. To achieve effective disease control, comprehensive impulsive measures are crucial. Our analysis shows that while increasing the pulse frequency and rates accelerates eradication, there exists an optimal frequency beyond which benefits diminish. Moreover, raising the pulse cure rate beyond a critical value yields limited gain, and a single additional high-coverage vaccination pulse can eliminate the infection. Thus, double impulsive strategies should be designed that considers cost-effectiveness and network heterogeneity.

Despite the valuable insights gained in this study, several limitations remain. One key challenge is our inability to derive an exact threshold that distinguishes between the extinction and persistence of the disease. Additionally, due to the complexity of our model, analyzing the existence and stability of endemic periodic solutions in the network-based epidemic model with impulsive strategies remains a difficult task. In future work, we aim to address these gaps through rigorous theoretical analyses. Furthermore, this study does not include a case study on infectious diseases such as hepatitis B, as real-world data and detailed information were unavailable. Moving forward, our research will focus on refining the impulsive epidemic model by incorporating more realistic factors and reliable data. One important future direction is to extend the numerical framework toward more realistic simulations,such as the following: (i) using real-world social networks to test the robustness of the thresholds and the resulting epidemic dynamics; (ii) exploring heterogeneous initial infection distributions, (e.g., concentrating initial cases in high-degree nodes); (iii) designing targeted intervention strategies that prioritize high-degree nodes for pulse vaccinations or screenings with treatments; and (iv) performing stochastic simulations to compare with the deterministic degree-based results. Another valuable future direction is to develop optimal impulsive control strategies for the proposed model under cost constraints. For example, regarding the spread of cyber propaganda, Chen et al. [35] proposed a methodology that combines the optimal impulsive control theory, which provides a valuable reference. To balance costs with epidemic control effectiveness, an optimal impulsive control problem will be formulated to determine the timing, intensity, or degree-targeting of vaccination and treatment. This line of work can also be extended to related propagation scenarios, such as malware or cyber propagation [36, 37], which significantly enriches the context and motivation to extend the current study. What's more, some network-based vaccination strategies in [38] can be integrated into this research framework of an epidemic model with double impulsive controls. It is also noted that a comparative study of different network information strategies is a promising extension [39]. This will enhance the model's applicability and effectiveness in practical disease control strategies.

Use of AI tools declaration

The authors declare they have not used Artificial Intelligence (AI) tools in the creation of this article.

Acknowledgments

This work was supported by the National Natural Science Foundation of China (62276094), the Natural Science Foundation of Hunan Province (2024JJ5088), the Major Scientific and Technological Innovation Platform Project of Hunan Province (2024JC1003), the China Scholarship Council (202306130070), the Postgraduate Scientific Research Innovation Project of Hunan Province under Grant CX20220433, and the Introduction of Talents Research Start-up Fund of Huai'an University (Z301B25557).

Conflict of interest

The authors declare that they have no known competing financial interests or personal relationships that could have appeared to influence the work reported in this paper.

References

1. J. Yang, L. K. Guan, Z. Chen, Y. S. Tan, Z. J. Liu, R. A. Cheke, Bifurcation analysis of a nonlinear pulse SIR model with media coverage, *Nonlinear Dyn.*, **111** (2023), 19543–19562. https://doi.org/10.1007/s11071-023-08869-x
2. S. Nayagam, M. Thursz, E. Sicuri, L. Conteh, S. Wiktor, D. L. Low-Beer, et al., Requirements for global elimination of hepatitis B: a modelling study, *Lancet Infect. Dis.*, **16** (2016), 1399–1408. https://doi.org/10.1016/S1473-3099(16)30204-3
3. Y. Y. Zhang, Z. T. Xu, Dynamics of a diffusive HBV model with delayed Beddington-DeAngelis response, *Chaos*, **15** (2014), 118–139. https://doi.org/10.1016/j.nonrwa.2013.06.005
4. T. Khan, S. Ahmad, G. Zaman, Modeling and qualitative analysis of a hepatitis B epidemic model, *Chaos*, **29** (2019), 103139. https://doi.org/10.1063/1.5111699
5. P. T. Karaji, N. Nyamoradi, Analysis of a fractional SIR model with General incidence function, *Appl. Math. Lett.*, **108** (2020), 106499. https://doi.org/10.1016/j.aml.2020.106499
6. G. Hussain, T. Khan, A. Zahri, G. Zaman, Ergodic stationary distribution of stochastic epidemic model for HBV with double saturated incidence rates and vaccination, *Chaos, Solitons Fractals*, **160** (2022), 112195. https://doi.org/10.1016/j.chaos.2022.112195
7. A. A. Raezah, A. Raouf, R. Zarin, A. Khan, Exploring the effectiveness of control measures and long-term behavior in Hepatitis B: An analysis of an endemic model with horizontal and vertical transmission, *Results Phys.*, **53** (2023), 106966. https://doi.org/10.1016/j.rinp.2023.106966
8. Z. Wang, Y. Moreno, S. Boccaletti, M. Perc, Vaccination and epidemics in networked populations-An introduction, *Chaos, Solitons Fractals*, **103** (2017), 177–183. https://doi.org/10.1016/j.chaos.2017.06.004

9. C. Nowzari, V. M. Preciado, G. J. Pappas, Analysis and control of epidemics: A survey of spreading process on complex networks, *IEEE Control Syst. Mag.*, **36** (2016), 26–46. https://doi.org/10.1109/MCS.2015.2495000

10. J. D. Cao, Y. Wang, A. Alofi, A. Al-Mazrooei, A. Elaiw, Global stability of an epidemic model with carrier state in heterogeneous networks, *IMA J. Appl. Math.*, **80** (2015), 1025–1048. https://doi.org/10.1093/imamat/hxu040

11. Y. C. Wu, Z. P. Zhang, L. M. Song, C. Y. Xia, Global stability analysis of two strains epidemic model with imperfect vaccination and immunity waning in a complex network, *Chaos, Solitons Fractals*, **179** (2024), 114414. https://doi.org/10.1016/j.chaos.2023.114414

12. S. Jafarizadeh, Convergence speed and robustness analysis of epidemic spreading processes with time-delay, *IEEE Trans. Netw. Sci. Eng.*, **10** (2023), 3818–3833. https://doi.org/10.1109/TNSE.2023.3274298

13. S. Lv, Y. Wang, C. Guo, L. B. Zhang, Effects of experts on the coupling dynamics of complex contagion of awareness and epidemic spreading, *Nonlinear Dyn.*, **112** (2024), 2367–2380. https://doi.org/10.1007/s11071-023-09146-7

14. A. L. Oestereich, M. A. Pires, N. Crokidakis, D. O. Cajueiro, Optimal rewiring in adaptive networks in multi-coupled vaccination, epidemic and opinion dynamics, *Chaos, Solitons Fractals*, **176** (2023), 114125. https://doi.org/10.1016/j.chaos.2023.114125

15. X. J. Fu, J. R. Wang, Dynamic behaviors and non-instantaneous impulsive vaccination of an SAIQR model on complex networks, *Appl. Math. Comput.*, **465** (2024), 128425. https://doi.org/10.1016/j.amc.2023.128425

16. Q. Q. Zhang, B. Tang, S. Y. Tang, Vaccination threshold size and backward bifurcation of SIR model with state-dependent pulse control, *J. Theor. Biol.*, **455** (2018), 75–85. https://doi.org/10.1016/j.jtbi.2018.07.010

17. G. R. Jiang, S. Y. Liu, L. Ling, Periodic solutions of an SIS epidemic model with fixed-time birth pulses and state feedback pulse treatments, *Int. J. Comput. Math.*, **91** (2014), 844–856. https://doi.org/10.1080/00207160.2013.818667

18. Q. Li, Y. N. Xiao, Analysis of a hybrid SIR model combining the fixed-moments pulse interventions with susceptibles-triggered threshold policy, *Appl. Math. Comput.*, **453** (2023), 128082. https://doi.org/10.1016/j.amc.2023.128082

19. L. Ding, P. Hu, Z. H. Guan, T. Li, An efficient hybrid control strategy for restraining rumor spreading, *IEEE Trans. Syst. Man Cybern.: Syst.*, **51** (2021), 6779–6791. https://doi.org/10.1109/TSMC.2019.2963418

20. Y. Y. Cheng, L. A. Huo, L. J. Zhao, Stability analysis and optimal control of rumor spreading model under media coverage considering time delay and pulse vaccination, *Chaos, Solitons Fractals*, **157** (2022), 111931. https://doi.org/10.1016/j.chaos.2022.111931

21. X. Wang, Y. D. Tao, X. Y. Song, Analysis of pest-epidemic model by releasing diseased pest with impulsive transmission, *Nonlinear Dyn.*, **65** (2011), 175–185. https://doi.org/10.1007/s11071-010-9882-4

22. Y. X. Xie, L. J. Wang, Q. C. Deng, Z. J. Wu, The dynamics of an impulsive predator-prey model with communicable disease in the prey species only, *Appl. Math. Comput.*, **292** (2017), 320–335. https://doi.org/10.1016/j.amc.2016.07.042

23. Y. F. Li, S. Huang, X. Y. Song, Global dynamic analysis of a nonlinear state-dependent feedback control SIR model with saturation incidence, *Eur. Phys. J. Plus*, **138** (2023), 636. https://doi.org/10.1140/epjp/s13360-023-04277-7

24. X. Z. Liu, P. Stechlinski, Pulse and constant control schemes for epidemic models with seasonality, *Nonlinear Anal.: Real World Appl.*, **12** (2011), 931–946. https://doi.org/10.1016/j.nonrwa.2010.08.017

25. X. Z. Liu, P. Stechlinski, Transmission dynamics of a switched multi-city model with transport-related infections, *Nonlinear Anal.: Real World Appl.*, **14** (2013), 264–279. https://doi.org/10.1016/j.nonrwa.2012.06.003

26. Q. C. Wu, M. Small, H. X. Liu, Superinfection behaviors on scale-free networks with competing strains, *J. Nonlinear Sci.*, **23** (2013), 113–127. https://doi.org/10.1007/s00332-012-9146-1

27. J. T. Yang, Z. C. Yang, Y. M. Chen, An SIS epidemic model in a patchy environment with pulse vaccination and quarantine, *Commun. Nonlinear Sci. Numer. Simul.*, **118** (2023), 107053. https://doi.org/10.1016/j.cnsns.2022.107053

28. V. Lakshmikantham, D. D. Bainov, P. S. Simeonov, Theory of impulsive differential equations, World Scientific, Singapore, 1989. https://doi.org/10.1142/0906

29. D. D. Bainov, P. S. Simeonov, Impulsive differential equations: periodic solutions and applications, Routledge, New York, 1993. https://doi.org/10.1201/9780203751206

30. S. J. Gao, D. H. Xie, L. S. Chen, Pulse vaccination strategy in a delayed SIR epidemic model with vertical transmission, *Discrete Contin. Dyn. Syst. – B*, **7** (2007), 77–86. https://doi.org/10.3934/DCDSB.2007.7.77

31. R. S. Varga, *Matrix Iterative Analysis*, Springer, New York, 2000. https://doi.org/10.1007/978-3-642-05156-2

32. X. Q. Zhao, *Dynamical Systems in Population Biology*, Springer-Verlag, New York, 2003. https://doi.org/10.1007/978-3-319-56433-3

33. R. K. Upadhyay, A. K. Pal, S. Kumari, P. Roy, Dynamics of an SEIR epidemic model with nonlinear incidence and treatment rates, *Nonlinear Dyn.*, **96** (2019), 2351–2368. https://doi.org/10.1007/s11071-019-04926-6

34. N. Chitnis, J. M. Hyman, J. M. Cushing, Determining important parameters in the spread of malaria through the sensitivity analysis of a mathematical model, *Bull. Math. Biol.*, **70** (2008), 1272–1296. https://doi.org/10.1007/s11538-008-9299-0

35. X. J. Cheng, L. X. Yang, Q. Y. Zhu, C. Q. Gan, G, Li, Impulse strategies for suppressing cyber propaganda with awareness, *IEEE Trans. Comput. Soc. Syst.*, **12** (2025), 2685–2695. https://doi.org/10.1109/TCSS.2024.3522889

36. X. J. Cheng, L. X. Yang, G. Li, Z. N. Ma, T. Q. Zhu, L. D. Wang, et al., Modeling and mitigating social engineering malware: integrating malware-opinion dynamics with optimal impulse control approaches, *IEEE Trans. Inf. Forensics Secur.*, **20** (2025), 12231–12244. https://doi.org/10.1109/TIFS.2025.3630005

37. X. J. Cheng, L. X. Yang, Q. Y. Zhu, C. Q. Gan, X. F. Yang, G. Li, Cost-effective hybrid control strategies for dynamical propaganda war game, *IEEE Trans. Inf. Forensics Secur.*, **19** (2024), 9789–9802. https://doi.org/10.1109/TIFS.2024.3468903

38. S. Chatterjee, A. N. Zehmakan, Effective vaccination strategies in network-based SIR model, *Chaos, Solitons Fractals*, **175** (2023), 113952. https://doi.org/10.1016/j.chaos.2023.113952

39. S. Chatterjee, A. N. Zehmakan, S. Rastogi, A novel room-based epidemic model: Quarantine, testing, and vaccination strategies, *Chaos, Solitons Fractals*, **177** (2023), 114297. https://doi.org/10.1016/j.chaos.2023.114297

Appendix

Proof of Lemma 3.1. From

$$\frac{\mathrm{d}N_{k_i}(t)}{\mathrm{d}t} = \mu - \mu N_{k_i}(t),$$

where $N_{k_i}(t) = S_{k_i}(t) + I_{k_i}(t) + R_{k_i}(t)$, it can be obtained that $N_{k_i}(t) = (N_{k_i}(0^+) - 1)e^{-\mu t} + 1$. Hence, $N_{k_i}(t) = 1$ for $i = 1, 2, \ldots, n$ under the given initial condition.

Observe that the pulse rates q_i and γ_i are in the interval $(0, 1)$. For System (2.1) with the initial condition, the nonnegativity of the solution $\mathbf{x}(t)$ can be guaranteed for all $t > 0$ provided that $\mathbf{x}(t)$ remains nonnegative when $t \neq (m + l - 1)T, t \neq mT$. Hence, we prove the claim that $\mathbf{x}(t) = \left\{(S_{k_i}(t), I_{k_i}(t), R_{k_i}(t))\right\}_{i=1}^{n}$ is nonnegative in each interval $(mT, (m+l)T) \bigcup ((m+l)T, (m+1)T], m \in \mathbb{Z}^+, 0 < l < 1$. Define the set $N = \{1, 2, \ldots, n\}$. If the above claim isn't true, then there exists a number $fir \in N$ such that $S_{k_{fir}}(t)$, $I_{k_{fir}}(t)$, or $R_{k_{fir}}(t)$ first approaches and crosses through the t-axis. We distinguish the following three cases:

Case 1. If $S_{k_{fir}}(t)$ first reaches and crosses through the t-axis at time $t_1 > 0$, then $S_{k_{fir}}(t_1) = 0$ and $\frac{\mathrm{d}S_{k_{fir}}(t)}{\mathrm{d}t}\Big|_{t=t_1} \leq 0$. Besides, $I_{k_{fir}}(t_1) + R_{k_{fir}}(t_1) = 1$ because of $N_{k_{fir}}(t_1) = 1$. Therefore, we get the following:

$$\begin{aligned}
\frac{\mathrm{d}S_{k_{fir}}(t)}{\mathrm{d}t}\Big|_{t=t_1} &= \mu - (1-\delta)\mu I_{k_{fir}}(t) - \lambda(k_{fir})S_{k_{fir}}(t)\frac{\Theta(t)}{1+\alpha\Theta(t)} - \mu S_{k_{fir}}(t)\Big|_{t=t_1} \\
&= \mu - (1-\delta)\mu I_{k_{fir}}(t_1) \\
&= \mu R_{k_{fir}}(t_1) + \delta\mu I_{k_{fir}}(t_1) \\
&> \delta\mu > 0,
\end{aligned}$$

which contradicts the assumption.

Case 2. If $I_{k_{fir}}(t)$ first reaches and crosses through the t-axis at time $t_1 > 0$, then $I_{k_{fir}}(t_1) = 0$, $\frac{\mathrm{d}I_{k_{fir}}(t)}{\mathrm{d}t}\Big|_{t=t_1} \leq 0$, and $I_{k_{fir}}(t) < 0$ in $(t_1, t_1 + \epsilon)$, where $\epsilon > 0$ is sufficiently small. Meanwhile, $S_{k_i}(t_1) \geq 0, I_{k_i}(t_1) \geq 0$ for $i = 1, 2, \ldots, n$ and $k_i \neq k_{fir}$. We can further prove $S_{k_{fir}}(t_1) > 0$ with the proof by contradiction. Assume $S_{k_{fir}}(t_1) = 0$, then $R_{k_{fir}}(t_1) = 1$. Besides, $\frac{\mathrm{d}S_{k_{fir}}(t)}{\mathrm{d}t}\Big|_{t=t_1} = \mu > 0$ holds. Like the

variable $I_{k_{fir}}(t)$, $S_{k_{fir}}(t)$ is also the first to reach and cross the t-axis at time t_1, which is consistent with the aforementioned case. Hence, we have $S_{k_{fir}}(t) \geq 0$ for $t > 0$. This suggests that the trajectory of $S_{k_{fir}}(t)$ must increase or remain in the interval $(t_1, t_1 + \epsilon)$, where $\epsilon > 0$ is sufficiently small. For these two possible situations, we conclude $\frac{\mathrm{d}S_{k_{fir}}(t)}{\mathrm{d}t}\Big|_{t=t_1} = 0$, which leads to a contradiction. Next, it's time to calculate the following:

$$\begin{aligned}\frac{\mathrm{d}I_{k_{fir}}(t)}{\mathrm{d}t}\Big|_{t=t_1} &= \lambda(k_{fir})S_{k_{fir}}(t)\frac{\Theta(t)}{1+\alpha\Theta(t)} - rI_{k_{fir}}(t) - \delta\mu I_{k_{fir}}(t)\Big|_{t=t_1} \\ &= \lambda(k_{fir})S_{k_{fir}}(t_1)\frac{\Theta(t_1)}{1+\alpha\Theta(t_1)} \\ &= \lambda(k_{fir})S_{k_{fir}}(t_1)\frac{\sum\limits_{k_i\neq k_{fir}}\omega(k_i)p(k_i)I_{k_i}(t_1)}{\langle k_i\rangle + \alpha\sum\limits_{k_i\neq k_{fir}}\omega(k_i)p(k_i)I_{k_i}(t_1)}.\end{aligned} \tag{A-1}$$

To better estimate the above Eq (A-1), it will be straightforward to discuss the following two sub-cases.

(1) There exits at least one variable $I_{k_i}(t_1) > 0, k_i \neq k_{fir}$ such that $\frac{\mathrm{d}I_{k_{fir}}(t)}{\mathrm{d}t}\Big|_{t=t_1} > 0$. Hence, our aim is directly achieved by contradiction.

(2) Provided that $I_{k_i}(t_1) = 0$ for $i = 1, 2, \ldots, n$ and $k_i \neq k_{fir}$, we are to deduce a contradiction. In fact, with the initial condition $I_{k_i}(t_1) = 0$ for all i, the equations for $I_{k_i}(t)$ in System (2.1) always have the zero solution $I_{k_i}(t) = 0, t > t_1, i = 1, 2, \ldots, n$. According to the assumption in this case, with the initial value $I_{k_{fir}}(t_1) = 0$, the equation for $I_{k_{fir}}(t)$ in System (2.1) has a solution that satisfies $I_{k_{fir}}(t) < 0$ in $(t_1, t_1 + \epsilon)$. For a small $\epsilon, \varepsilon > 0$, in the domain $D : t_1 < t < t_1 + \epsilon, -\varepsilon < I_{k_i}(t) < \varepsilon, i = 1, 2, \ldots, n$, it follows from the continuity of $\mathbf{f}(\mathbf{x}(t))$ and $\frac{\partial \mathbf{f}(\mathbf{x}(t))}{\partial \mathbf{x}(t)}$ that the right-hand side of System (2.1) is locally Lipschitz continuous. Since $\mathbf{f}(\mathbf{x}(t))$ is locally Lipschitz continuous with respect to $\mathbf{x}(t)$, there exists a unique solution $\mathbf{x}(t)$ of System (2.1) locally in the interval $(t_1, t_1 + \epsilon)$. In consequence, the results obtained above contradict the uniqueness of the solution of System (2.1) starting from the initial value $I_{k_{fir}}(t_1) = 0$.

Case 3. If $R_{k_{fir}}(t)$ first reaches and crosses through the t-axis at time $t_1 > 0$, then $R_{k_{fir}}(t_1) = 0$ $R_{k_{fir}}(t) < 0$ in $(t_1, t_1 + \epsilon)$, where $\epsilon > 0$ is sufficiently small. Based on the above result, we have $\frac{\mathrm{d}R_{k_i}(t)}{\mathrm{d}t} \geq -\mu R_{k_i}(t)$, which implies $R_{k_i}(t) \geq 0$. Hence, a contradiction arises in the interval $(t_1, t_1 + \epsilon)$.